2010-draft

Self-Ignition delay Prediction in PCCI direct injection diesel engines using multi-zone spray combustion model and detailed chemistry

A.S. Kuleshov
Bauman Moscow State Technical University, Russia

A.V. Kozlov
East-Ukrainian National University, Ukraine

K. Mahkamov
Durham University, UK

.

ABSTRACT

A multi-zone direct-injection (DI) diesel combustion model has been implemented for full cycle simulation of a turbocharged diesel engine. The above combustion model takes into account the following features of the spray dynamics:

- the detailed evolution process of fuel sprays;
- interaction of sprays with the in-cylinder swirl and the walls of the combustion chamber;
- the evolution of a Near-Wall Flow (NWF) formed as a result of a spray-wall impingement as a function of the impingement angle and the local swirl velocity;
- interaction of Near-Wall Flows formed by adjacent sprays;
- the effect of gas and wall temperatures on the evaporation rate in the spray and NWF zones.

In the model each fuel spray is split into a number of specific zones with different evaporation conditions including in zones formed on the cylinder liner surface and on the cylinder head. The piston bowl in the modelling process is assumed to have an arbitrary axi-symmetric shape. The combustion model considers all known types of injectors including non-central and side injection systems. A NOx calculation sub-model uses detailed chemistry analysis which considers 199 reactions of 33 species. A soot formation calculation sub-model used is the phenomenological one and takes into account the distribution of the Sauter Mean Diameter in injection process. The ignition delay sub-model implements two concepts. The first concept is based on calculations using the conventional empirical equations. In the second approach the ignition delay period is estimated using relevant data in the calculated comprehensive 4-D map of ignition delays. This 4-D map is developed using CHEMKIN detailed chemistry simulations which take into account effects of the temperature, the pressure, the Air/Fuel ratio and the EGR. The above approach is also planned to be used in future for calculations of ignition delays in diesel engines fuelled by bio-fuels. The model has been validated using published experimental data obtained on high- and medium-speed engines. Comparison of results demonstrates a good agreement between theoretical and experimental sets of data.

The above sub-models were integrated into DIESEL-RK software, which is a full-cycle engine simulation tool, allowing more advanced analysis of PCCI and HCCI diesels.

INTRODUCTION

In direct-injection diesels the combustion process together with NOx and PM emission formations is very sensitive to the engine design and operational parameters such as the sprayer design and its location, the shape of the piston bowl, the swirl intensity, strategy of the EGR use and the fuel injection profile including multiple electronically controlled injection.

One of the ways to lower NOx emissions is the modification of the combustion process so that more of burning occurs under lean conditions, resulting in reduction of local combustion temperatures and therefore in less NOx formations. Lowering the combustion temperature also allows simultaneously reduce soot formation. One method of achieving overall lean combustion is implementation of the Premixed Charge Compression Ignition (PCCI) or Homogeneous Charge Compression Ignition (HCCI) in which the entire

fuel and air charge is premixed prior to the start of combustion. The PCCI/HCCI processes have been the focus of numerous research investigations because these provide low levels of NOx without an increase in the PM formation and in the fuel consumption. There are a number of challenges for implementation of the PCCI/HCCI mode over the whole engine operating range because of the high rate in the pressure rise and problems associated with a controlled start of combustion. So at the stage of computational analysis of engines the suitable mathematical model and the associated computer code should be able to support both the conventional engine combustion and PCCI/HCCI combustion mode to make it possible to use such the code for computer optimization of the engine control parameters over the whole operating range.

Due to a great number of variables and their possible combinations, an experimental search for the optimal combination of variable parameters can be a very time and labour consuming process. Suitable numerical simulations using an appropriate model coupled with a computational optimization method can effectively pinpoint effective ways of engine improvement.

Currently there are following three categories of diesel engine simulation models:

- Zero-dimensional single-zone combustion models;
- Quasi-dimensional multi-zone combustion models;
- Multi-dimensional models (CFD).

Although CFD models possess, in principle, the ability to simulate fluid flow/heat transfer/chemical reactions as integral phenomena, in practice their application is limited by: a) the capacity of current computer hardware to handle small-scale phenomena in an acceptable period of time; b) inadequacy in current scientific knowledge of turbulence, two-phase flow and chemical reactions, especially when the above three are simultaneously presented in the physical processes. So, application of “CFD only” approach for optimization of diesel-engine working processes is currently prohibitively expensive in most cases.

The choice of the thermodynamic engine model together with a quasi-dimensional multi-zone model of combustion capable to reflect specific features of conventional and PCCI diesel combustion is determined by requirements for both the high accuracy and the high computational speed, because the total number of engine simulation sessions during the engine optimization process over its whole operating range reaches several thousands.

The earlier published multi-zone diesel spray combustion model [1-3], named the RK-model includes three independent emission calculation sub-models, namely for the NOx formation calculations which is based on the Zeldovich’s scheme [4] developed by Zvonov [5]; for the soot formation calculations developed by Razleytsev [6] and for the advanced NOx formation calculations which is based on the Detail Kinetic Mechanism (DKM) for correct prediction of NO emission in engine with large EGR, multiple injection and PCCI/HCCI. The DKM includes 199 reactions with 33 species and is built on the kinetic scheme by Basevich [5, 7, 8, 9]. Soot and NOx formation processes are simulated using separate procedures run after combustion modeling is complete. The main equations of the RK-model were derived by Razleytsev in 1990-1994. This method afterwards was further modified and developed by Kuleshov [1-3].

The RK-model takes into account details of evolution of each fuel spray and those of near-wall flows formed by sprays. The model also accounts for interaction between the sprays and the swirl, as well as interaction between the near-wall flows, created by adjacent sprays. The following parameters can be varied during the modeling process:

- the piston bowl shape and the sprayer location;
- the swirl intensity;
- the number, the diameter and orientation of the sprayer nozzles;
- the injection profile shape and any multiple injection.

The above features of the RK-model allow us to accurately predict the diesel combustion process and formation of emissions over the whole operating range.

A more detailed description of the RK-model is presented in [1, 2, 3, 35, 53]. The present paper describes additional features of the RK-model developed and integrated into the model with a purpose to improve the accuracy of the heat release prediction in diesels with PCCI process.

GENERAL PRINCIPLES OF SPRAY MODELLING

The theoretical background of the model is based on the method developed in [6] in which the fuel spray injected into the combustion chamber of the engine is split into a number of specific zones. This is necessary in order to take into account the following features of the fuel spray evolution:

- differences in the fuel droplet evaporation conditions present in the various spray zones;
- fuel redistribution between the different zones in the process of free spray movement and during its interaction with a wall;
- interaction of the fuel sprays with the walls of the piston bowl and when fuel reaches the cylinder liner and the cylinder head surfaces;
- the effect of the wall temperature on the fuel evaporation rate in the near-wall zones;
- interaction of adjacent sprays in the near-wall flows.

The spray evolution passes through the following three stages:

- Initial formation of the dense axial flow;

- The main stage of the cumulative spray evolution;
- The period of the spray interaction with the combustion chamber walls and fuel distribution on the walls.

During the stage of the spray's initial formation breakup of the liquid spray starts in the vicinity of the nozzle. High-speed fuel droplets move rapidly towards the spray tip creating a body of a conical shape. There is interaction between droplets and thus new droplets catch up and combine with the droplets formed earlier. The density distribution of the droplets and their diameters in the spray's cross section plane reduce rapidly with the increase of the distance from the spray axis. Therefore the droplets close to the jet's boundary are slowed down more quickly than those moving close to the axis. These droplets, which are close to the external surface of the spray, gradually fall behind and separate from the droplets moving in the spray's core.

At the main evolution stage, the axial flow is also slows down with the fuel density growing in the forward front side because of the surrounding gas resistance. Newly injected fuel portions join the axial flow, travel through the spray's core, reach and extend the front of the spray. This results in the extended axial core with the increased density and droplet velocity in the middle of the spray [10]. The core is surrounded by a relatively dilute outer sleeve formed by the slowed down droplets. The corresponding scheme of the diesel fuel spray is presented in Fig. 1.

Figure 1. The scheme of the diesel fuel spray showing the concentration of fuel droplets and their paths.

The instance which separates the initial and main stages of the spray evolution corresponds to the moment of time when the axial flow close to the spray tip starts to deform and break up, forming a condensed mushroom-shaped forward front. As the spray moves on, constant breakup of the spray's forward section [11] takes place and the front is renewed by the newly injected fuel portions [12, 13]. The slowed down droplets move away from the breaking front to the surrounding environment. The moving spray also carries some of the surrounding gas with it. The gas velocity in the surrounding environment is considerably lower than that of the spray. Meanwhile the gas inside the axial core is rapidly accelerated to the velocity close to that of the droplets [14]. In the cross section plane the diameter of the spray's core is about 0.3 of the spray's outside diameter.

In accordance with [6], the current position and the velocity of an Elementary Fuel Mass (EFM) injected during a small time-step and traveling from the injector towards the spray tip are related as

$$\left(\frac{U}{U_o}\right)^{3/2} = 1 - \frac{l}{l_m} \qquad (1)$$

where: l is the current distance between the injector's nozzle and the location of the EFM; $U = dl/dt_k$ is the current velocity of the EFM; t_k is the travel time for the EFM to reach a distance l from the injector's nozzle; U_o is the initial velocity of the EFM at the nozzle of the injector and l_m is the EFM's penetration distance.

As an illustration, Fig. 2 presents the variation of the spray's parameters l, l_m, U and U_m as functions of time during the fuel spray evolution process in a medium speed diesel engine.

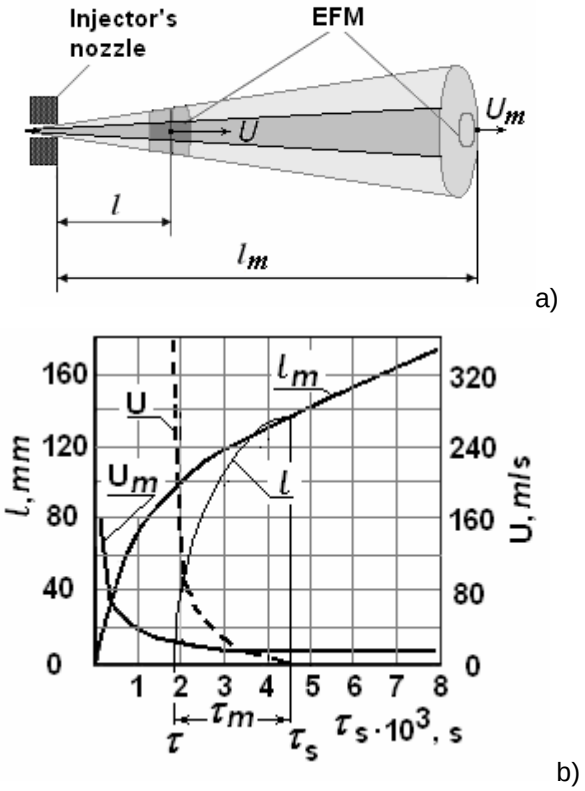

Figure 2. The simplified sketch of the spray (a) and variations of spray's parameters l, l_m, U and U_m as functions of time during fuel spray evolution process (b).

Upon termination of the fuel evolution there is still some fuel in its axial core which was supplied at the final injection stage. At the initial combustion stage the flame is unable to break up the fuel spray's condensed core [15, 16, 6] which explains the fact that the sprays continue to move to the combustion chamber sidewalls during injection even after the fuel ignition takes place. By the end of the fuel supply process a considerable fraction of the fuel cycle portion is accumulated near the walls. This takes place both in diesels with compact combustion chambers and in engines with wide piston

bowls (Hesselman). The interaction of fuel sprays with chamber walls was studied by many researchers and results are presented in numerous publications [17-24]. Having analyzed different sources of data, Razleytsev proposed the following model of the fuel spray interaction with a wall. After reaching the wall, the spray is spread over its surface in every direction forming the near-wall flows. The near-wall flow moving upwards quickly reaches a clearance between the piston and the cylinder head and spreads on the piston crown as well as on the cylinder head surface. A typical photo-record of the evolution of the spray in the combustion chamber is shown in Fig.3. A part of fuel can reach the cylinder liner. Analysis of experimental data has shown that characteristics of flows moving along the wall in different directions are similar to those obtained for a freely moving spray, but the velocity levels are lower and depend on the flow directions. The reduction in the flow velocity along the wall surface is caused by the corresponding hydrodynamic resistance.

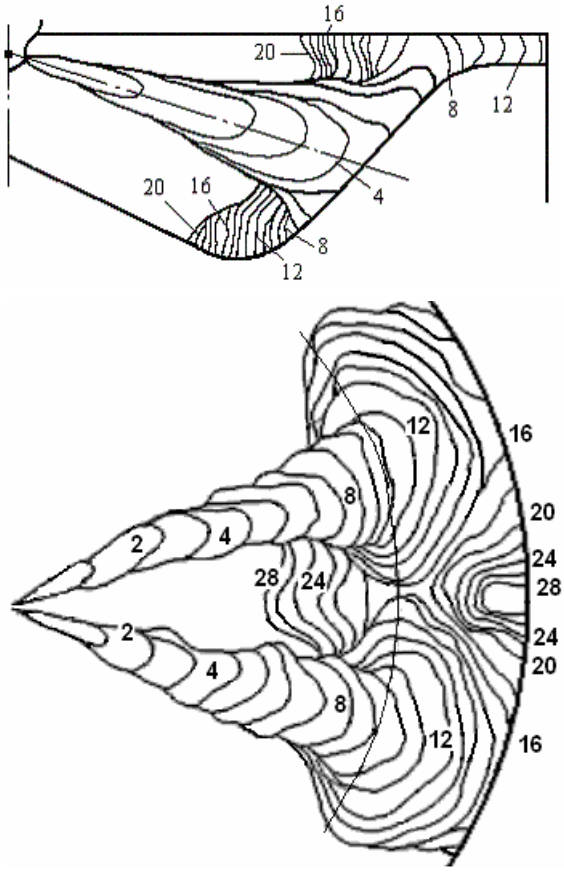

Figure 3. Photo-record obtained by Koptev, Gavrilov [25] and Plotnikov. Fuel was injected into the bomb with the piston model. Nozzles: 7 x 0.4 mm. Recording speed is 3700 frames/sec. The numbers on the diagram correspond to the frames during recording.

The above mentioned similarity between evolutions of near-wall flows and of the free sprays provides the basis for the application of the same computational procedures to the near-wall flows and the free sprays. The assumption that the velocity of the elementary fuel portion traveling along the wall is similar to the fuel velocity of the flow from a sprayer makes it possible to apply conventional mathematical relations for the simulation of the flows in the near-wall zones.

As the spray reaches the wall, the forward front fuel enters the near-wall flow zone. The spray trajectory and, therefore, the time, the place and the impingement angle are determined taking into account the swirl effect. The process of interaction between the spray and the wall is extremely complex phenomena. The following calculation scheme of the spray and of the NWF evolutions is proposed:

- When the spray's forward front impinges the wall an initial conical condensed gas-fuel layer forms on the wall with its boundaries defined by the intersection of the conical fuel spray and the wall's surface (zone 4 in the Fig. 8).
- During the further impingement of the fast fuel spray front fuel spreads out the initial boundaries of the near-wall layer.
- When the high-speed axial flow of the spray reaches the wall than thickness of the near-wall layer increases, its boundaries extend and a part of fuel flows above this layer outwards from its center.
- The shape of the near-wall layer on the wall and its spreading rate in various directions depends on the spray impingement angle and the air swirl effect.

The partial solution of the Equation 1 can be found as

$$3l_m\left[1-\left(1-\frac{l}{l_m}\right)^{0.333}\right]-U_0 t_k = 0 \qquad (2)$$

where t_k is the time of the EFM movement from the nozzle to the distance l. When the EFM reaches the spray tip then $l = l_m$, $t_k = t_m$ and

$$l_m = U_o\ t_m / 3. \qquad (3)$$

From Equations 1, 2, 3 it follows that

$$U = U_0\left(1-t_k/t_m\right)^2\ ; \qquad (4)$$

$$l = l_m\left[1-\left(1-t_k/t_m\right)^3\right]\ . \qquad (5)$$

Parameters of the spray tip are calculated using empirical equations by Lyshevsky [26]. These equations use the following dimensionless parameters:

$$We = U_{0m}^2\, d_n\ r_f / s_f\ ; \qquad (6)$$

$$M = Oh^2 = m_f^2 / \left(r_f\, d_n\, s_f\right)\ ; \qquad (7)$$

$$Э = t_s^2\, s_f / \left(r_f\, d_n^3\right)\ ; \qquad (8)$$

$$r = r_{air} / r_f \qquad (9)$$

Here U_{0m} is the average injection velocity, d_n is the nozzle hole diameter, r_f is the fuel density, r_{air} is the air density, s_f is the fuel surface density, m_f is the dynamic viscosity coefficient of fuel, t_s is the current time from the start of injection.

Evolution of the free spray consists of two main phases: a) the initial phase of pulsation evolution and b) the main phase of cumulative evolution. The boundary between these two phases is defined in terms of length (l_g) and time (t_g):

$$l_g = C_s\, d_n\, We^{0.25} M^{0.4}\, r^{-0.6}; \quad (10)$$

$$t_g = l_g^2 / B_s; \quad (11)$$

$$B_s = d_n U_{0m} We^{0.21} M^{0.16} / \left(D_s \sqrt{2}\, r\right); \quad (12)$$

where C_s = 8.25÷8.85 and D_s = 4.5÷5 for diesel cylinder conditions. The spray tip penetration length in the initial (index *a*) and the main (index *b*) phases is calculated using the following empirical equations [6]:

$$l_a = A_s \Im^{0.35} exp\left[-0.2\left(t_s / t_g\right)\right]; \quad (13)$$

$$l_b = B_s^{0.5} t_s^{0.5}; \quad (14)$$

where $A_s = 1.22\, l_g\, \Im_g^{-0.35}$. Here the parameter $\Im_g$ is calculated using Equation 8 and assuming that $t_s = t_g$. The form of Equation (14) is close to that derived by Kuo [27] and Hiroyasu [28]. Equations 6-14 with D_s = *const* were obtained by Lyshevsky for medium-speed diesels. To make this model suitable for high-speed diesels with small injector nozzles, the following expression for D_s was derived in the current investigation:

$$D_s = 14.21 / D_f \quad (15)$$

where

$$D_f = \begin{Bmatrix} 2.9, & if\ d_n \ge 0.3 \\ 2.9\left(a \cdot d_n^3 + b \cdot d_n^2 + c \cdot d_n + d\right), & if\ d_n < 0.3 \end{Bmatrix}; \quad (16)$$

Here d_n is the nozzle diameter in millimeters; *a*=9.749; *b*=7.45; *c*= -7.21; *d*=2.224. Equations 15 and 16 have been derived as a result of analysis of experimental data on the dependence of the fuel spray penetration distance from the value of the nozzle diameter and the injection pressure presented in [29–32]. In these investigations the diameter of the nozzles and injection pressures were varied from 0.11 to 0.45 mm and from 300 to 1200 bar, respectively.

The Equations 6-16 provide correct results for the wide range of spray nozzle diameters and for different injection pressures.

The spray angle is calculated as follows:

$$g_a = 2Arctg\left(E_s We^{0.35} M^{-0.07} \Im^{-0.12} r^{0.5} e^{0.07 t_s / t_g}\right); \quad (17)$$

$$g_b = 2Arctg\left(F_s We^{0.32} M^{-0.07} \Im^{-0.12} r^{0.5}\right) \quad (18)$$

where $E_s = 0.932 F_s We^{-0.03} \Im_g^{0.12}$ and parameter $\Im_g$ is calculated using Equation 8 and assuming that $t_s = t_g$, F_s = 0.0075÷0.009 for diesel cylinder conditions. Fig. 4 shows comparison of free spray contours and angles obtained experimentally and using different simulation methods.

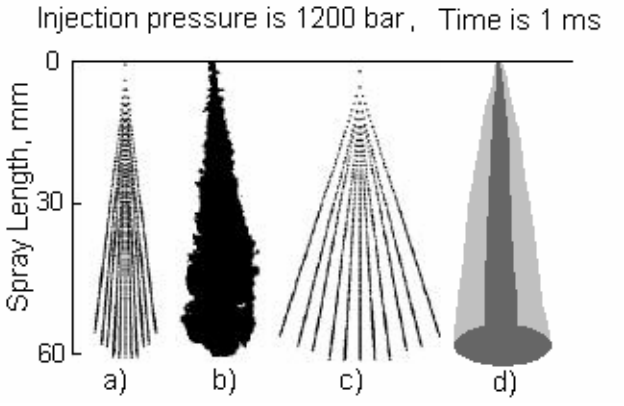

Figure. 4. The free spray contours obtained by different ways: a) calculated by Reitz and Bracco using KIVA [33]; b) measured by Dan [34]; c) calculated by Jung and Assanis [35] using Hiroyasu and Arai equations [36]; d) calculated using Equations 17 and 18.

If a swirl with an angular velocity ω exists in the combustion chamber then the spray is deformed and its axis is deflected by some distance *y* in the tangential direction inside the chamber, as shown in Fig. 5. The deformation of the initial conical form of the spray is characterized by the parameters *y, y_3, y_4* and *r*. The local tangential air velocity is:

$$W_t = c\, R_s\, p\, n R / 30; \quad (19)$$

where R_S = ω / ω_C is the swirl ratio, *n* is the engine speed, R is the current radius, χ is the swirl damping factor depending on CA. Tangential velocity of the EFM in the swirl direction U_t is defined by the equation presented in [37]:

$$dU_t / dt = A_{wt}\, W_t^{1.5}; \quad A_{wt} = 0.75 C\, r\, n^{0.5} d_{32}^{-1.5} \quad (20)$$

Here $C \approx 5$ is empirical coefficient, ν is the air kinematical viscosity, $d_{32} = 1.7\, d_n\, M^{0.0733} \left(We\ r\right)^{-0.266}$ is the Sauter Mean Diameter of droplets. The change in the deflection distance of the spray axis at each time step due to the swirl is defined as $\Delta y = U_t\ \Delta t\ \cos b$, where Δt is the time step, b is the angle between the line tangential to the spray axis in its starting point and the current end the fuel spray's axis. The geometry of the deformed spray is also defined in terms of y_3 and y_4 which are calculated for each time step as

$$dy_3 = -C_{30} A_{wt} (W_t - U_t)\ \Delta t\ \cos b;$$
$$dy_4 = C_{40} A_{wt} (W_t - U_t)\, \Delta t\ \cos b \quad (21)$$

where $C_{30} \approx 0.2$ and $C_{40} \approx 1.6$ are empirical coefficients.

After the fuel spray impinges the wall, the dense near-wall flow consisting of the fuel droplets and air, is formed. The NWF expands on the wall's surface in all directions. The shape of the NWF on the wall depends on impingement angles: g_j, (j = 1, 2, 3, 4), see Fig. 5.

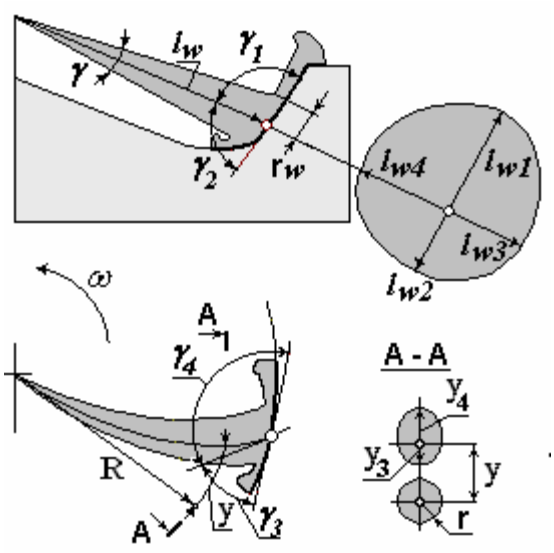

Figure. 5. Schematic diagram of the fuel spray and the near-wall flow in the air swirl.

Impingement angles are calculated taking into account the effect of the air swirl and the shape of the piston bowl in the point of impingement. Dimensions of the NWF formation in each directions l_{wj} (j =1, 2, 3, 4) are defined as follows:

$$l_{wj} = K_j \, B_{sw}^{0.5} \, t_w^{0.5}; \qquad t_w = t_s - t_{sw}; \qquad (22)$$

$$B_{sw} = \left[\left(f + 0.08\, K_{j\max}\right) / K_{j\max}\left(l_{b\max} - l_w\right)\right]^2 / \left(t_{s\max} - t_{sw}\right)$$

where f = 0.6 is the factor of losses due to impingement, t_{sw} is the time of impingement[1], $t_{s\,max} = t_{inj} + (0.3 \div 0.5)10^{-3}$ (in seconds) is the time corresponding to the completion of the spray evolution, $l_{b\,max}$ is the free spray length when the spray evolution is completed, l_w is the travel distance of the spray prior to impingement.

On the basis of experimental photo-records made by Gavrilov, Koptev, and Plotnikov the following expression for the NWF spot dimensions as function of impingement angles γ_1, γ_2, γ_3, γ_4, (see Fig. 5) was derived by Gavrilov [25]:

$$K_j = \sqrt{sing_1\, sing_3} + 1.2\left(1 - sing_j\right) - 2\left(cosg_j\right)^3; \qquad (23)$$

$$K_{j\,max} = MAX\left(K_1, K_2, K_3, K_4\right).$$

The time of the wall impingement t_{sw} is determined by Equations 13, 14 and 20 taking into account the 3-D coordinates of the spray's tip and the piston displacement.

Comparison of calculations of the spray tip penetration and the NWF boundaries evolution, using Equations 6-23, and the experimental data is presented in Fig. 6. In this figure the experimentally measured values are labeled as dots and the frame numbers correspond to those in Fig. 3. Subscript "*free*" is used for the case of free spray evolution.

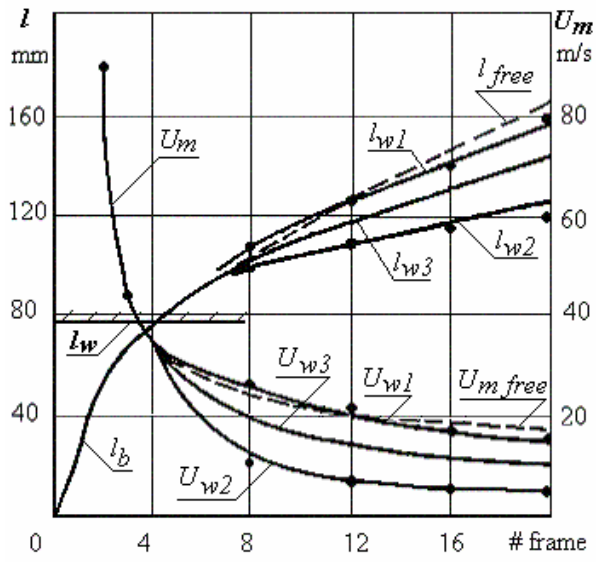

Figure. 6. Spray evolution phenomena for conditions in a turbocharged diesel: S/D=300/230, RPM=750, m_f = 0.62 g. U_{wj} are velocities on the corresponding NWF boundaries. Data was obtained by Razleytsev [6].

A special Fuel Spray Visualization (FSV) computer code has been developed for visualization of the fuel spray evolution. Spray images presented in Fig. 7 are obtained using this code. Comparison of the calculated image of the spray and the NWF evolution with the experimental photo-record is shown in Fig. 7. Frame "b" shows pictures of the near-wall flows obtained by superposition of recorded frames with the sprays images artificially removed. It can be seen that there is a good match between shapes of the NWF formations obtained experimentally and numerically.

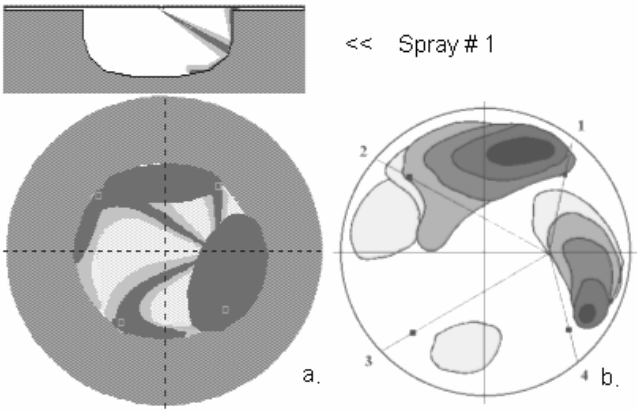

Figure 7. Comparison of the calculated image of the sprays and NWF evolution: (a) numerical results (b) experimental results on the tractor diesel: S/D =140/120, RPM=1800.

[1] In fact the wall impingement process starts at the instance when the spray's front contacts an oblique surface of the piston and is completed when the full transition of fuel from the front in the core of the NWF takes place. In this brief schematic description of the RK-model, the detailed algorithm is not presented.

DISTRIBUTION OF FUEL IN A SPRAY

A fuel spray, which is injected into the combustion chamber, is divided into 7 characteristic zones as shown in Fig. 8. Each zone has specific conditions of evaporation and burning and these conditions are uniform within an individual zone.

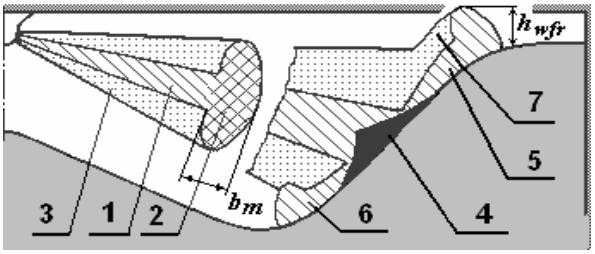

Figure 8. Characteristic zones of the diesel spray.

During the time prior to the jet impingement only three zones are considered in the spray. These are: 1 – the dense conical core, 2 – the dense forward front, 3 – the dilute outer sleeve. The near-wall flow which is formed by the spray impingement is inhomogeneous in the structure, in the density and in the temperature, which makes the calculation of fuel evaporation very difficult. It is therefore convenient to split the near-wall flow into several zones with the averaged heat and mass transfer coefficients. This is done by analogy with the free spray division into typical zones. After the impingement, new zones are considered as follows: 4 – the axial conical core of the NWF, 5 – the dense core of the NWF on the piston bowl surface, 6 – the dense forward front of the NWF, 7 – the dilute outer zone of the NWF. If during its evolution, the spray reaches the surface of the cylinder liner and/or the head of the cylinder then it is necessary to introduce additionally two corresponding zones. The depth of the spray forward front is calculated as:

$$b_m = A_m \, l \, F_s \, We^{0.32} M^{-0.07} \, r^{0.5} \qquad (24)$$

where $A_m \approx 0.7$ is an empirical coefficient. The sequence of the fuel distribution calculation in the zones at each moment of time t_s (varying from 0 up to $t_{s\,max}$ with some increment) is as follows:

1. The fuel fraction s_s injected into the cylinder is determined using the injection profile $s = f(t)$.
2. The spray length l at the current time t_s can be calculated using Equations 13 and 14.
3. The time corresponding to the start of injection of the EFM which travels the distance l from the nozzle to the front of the spray can be calculated as: $t = t_s - t_m$, where t_m is defined using Equation 3.
4. The fuel fraction s_t injected into the cylinder at time t is determined from the injection profile $s = f(t)$.
5. The distance between the nozzle and the section behind the spray front is $l_k = l - b_m$, see Fig. 8 and Equation 24.
6. The time of injection of the EFM which reaches the section behind the spray front t_k is calculated using Equations 3, 5, 13 and 14.
7. The fuel fraction s_k injected into the cylinder at the time t_k is determined from the injection profile $s = f(t)$.

Distribution of fuel among the spray zones is determined at each time step using the following equations:

in core: $$s_{core} = (s_s - s_k)(1 - 0.1 l_k / l); \qquad (25)$$

in front: $$s_{front} = 0.8\,(s_k - s_t) A; \qquad (26)$$

in dilute outer sleeve:

$$s_{env} = s_t + 0.2(s_k - s_t) + (s_s - s_k)\,0.1\,l_k / l; \qquad (27)$$

in the NWF: $$s_W = 0.8\,(s_k - s_t)\,(1 - A) \qquad (28)$$

where A = 1 prior and A=0 after the wall impingement.

After the spray impinges the wall, an additional control section $l_k = l_w$ is introduced to determine the fuel fractions allocated in the zones of the NWF: the outer section of the NWF $s_{w\,env}$, the core of NWF $s_{w\,core}$ and the front of NWF $s_{w\,fr}$. If the NWF formation reaches the piston crown, then the fuel fraction in this zone s_{crown} is determined as

$$s_{crown} = s_W \, V_{crown} / V_W . \qquad (29)$$

If the NWF forward front reaches the cylinder head surface as shown in Fig. 9, then the fuel fraction in the cylinder head zone s_{head} is determined as

$$s_{head} = s_{w\,fr} \, V_{head} / V_{w\,fr}; \quad s_{w\,fr} = s_{w\,fr} - s_{head}. \qquad (30)$$

The fuel-air mixture allocation on the cylinder head surface is calculated as:

$$h_{w\,fr} = F_{sw} \, l_{w1} \, We^{0.32} M^{-0.07} \, r^{0.5} > h_{clr}, \qquad (31)$$

where $h_{w\,fr}$ is the height of the NWF forward front, see Fig. 9, h_{clr} is the piston-head clearance which varies with CA and $F_{sw} \approx 1.5\,F_s$.

If the NWF formation reaches the cylinder liner, the fuel fraction in the liner zone s_{liner} is calculated as

$$s_{liner} = s_W \, V_{liner} / V_W \; ; \; C_{liner} = 1 - V_{liner} / V_W . \qquad (32)$$

The other fuel fractions in the zones of the NWF are:

$$\begin{aligned} s_{w\,core} &= s_{w\,core} \, C_{liner}; \\ s_{w\,fr} &= s_{w\,fr} \, C_{liner}; \quad s_{w\,env} = s_{w\,env} \, C_{liner}; \\ s_W &= s_{w\,core} + s_{w\,fr} + s_{w\,env}. \end{aligned} \qquad (33)$$

If two adjacent near-wall flows mix with each other, then the fuel fraction in the mixing zone s_{cross} is calculated as

$$s_{cross} = V_{cross} / V_W \; (s_{w\,core} + s_{w\,fr} + A_{w\,env} \, s_{w\,env}); \qquad (34)$$

where $A_{w\_env} \approx 0.5$ and this is the coefficient taking into account a decrease in the NWF formation due to mixing of adjacent near-wall flows. The fuel fractions in other zones of the NWF are

$$s_{wcore} = s_{wcore}\left(1 - V_{cross}/V_W\right);$$
$$s_{w\,fr} = s_{w\,fr}\left(1 - V_{cross}/V_W\right); \qquad 35)$$
$$s_{wenv} = s_{wenv}\left(1 - A_{wenv}\,V_{cross}/V_W\right).$$

Overall, the fuel fraction in the NWF formation due to one spray is

$$s_W = s_{wcore} + s_{w\,fr} + s_{wenv}.$$

Volumes of the characteristic zones, namely V_W, V_{crown}, V_{head}, $V_{w\,fr}$, V_{liner}, V_{cross} in Equations 29–35, are calculated as volumes of corresponding three-dimensional geometrical figures separated from each other by suitable planes or other figures.

Each spray is simulated as a separate single spray and the fuel fractions from all sprays are added for every zone.

Results of calculations of the fuel distribution in the zones for different diesels are presented in Fig. 9 and Fig. 10. All calculations were carried out with identical sets of empirical constants.

If the sprayer is not central or spray angles are not identical, as it shown in Fig. 9, each spray is simulated independently with corresponding specific swirl effect and angles of impingement. Fig.9 presents different phases of the spray evolution and wall impingement. The period from the start of the first spray impingement to the end of the last spray impingement is 5 CA deg (from 360^0 up to 365^0). Fig. 9 also presents results of calculation of the fuel fractions in different zones from all seven sprays. In a compact combustion chamber of a heavy-duty truck diesel there is no sufficient space for free evolution of the near-wall flows. Mixing of some near-wall flows starts already in the middle of the injection process and it can be observed in the frame *b* in Figure 9. A noticeable rise in the fuel fraction in the zones of the NWF mixing takes place at the end of the injection process, see frame *c* in Fig. 9 (s_{cross}). This has a negative effect and the amount of the fuel in the zone of the dilute outer sleeve is reduced (curve: $s_{env}+s_{wfr}+s_{wenv}$) and the combustion rate decreases.

If the sprayer is central and all the spray angles are identical, as it shown in Fig. 10, only one spray is simulated and then corresponding results obtained are multiplied by a number of sprays. Usually, in medium-speed diesels with the Hesselman combustion chamber, there is more space for free spray evolution, therefore more fuel is distributed to the zones with good evaporation conditions, namely the dilute outer sleeve and the forward front. Fig. 10 shows that the fuel fraction in these zones exceeds 80% (the curve $s_{env}+s_{w\,fr}+s_{wenv}$) whereas in diesels with a compact combustion chamber this fraction usually lies in the range 60-70%.

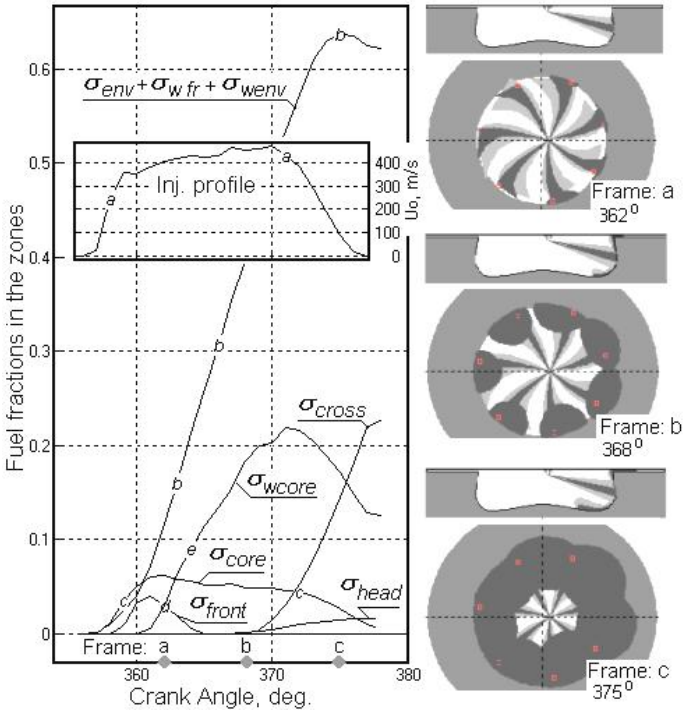

Figure. 9. Results of simulations of the fuel allocation in the characteristic zones in the combustion chamber of a truck diesel: S/D=140/130 and RPM=1700.

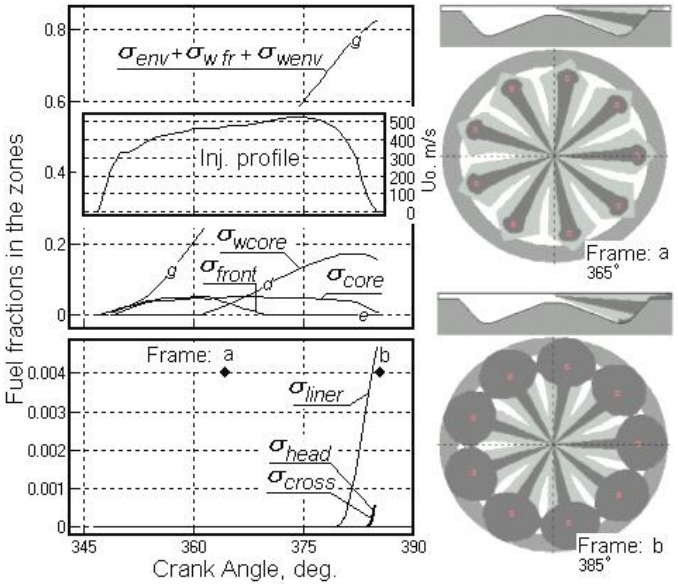

Figure. 10. Results of simulations of the fuel allocation in the characteristic zones in the combustion chamber of a medium speed diesel: S/D=260/260, the spray angle is 160^0, RPM=1000 and BMEP=15 bar.

Due to the sharp angles of the spray and of the wall impingement, the NWF expands rapidly in the radial direction and can reach the cylinder liner surface as it shown in Fig. 10 (frame *b* and curve s_{liner}). There are poor evaporation conditions in the liner zone and it is essential to eliminate or reduce the fuel fraction reaching

this zone. This is especially important for engines with a very shallow piston bowl. The example shown in Fig. 10 demonstrates that the very small fuel fractions are allocated in the NWF mixing zone, in the liner zone and in the cylinder head zone and this is due to the small amount of the injected fuel.

FUEL EVAPORATION MODELING

During injection and evolution of sprays the rate of combustion is limited mainly by the rate of the fuel evaporation. The zones of intensive heat exchange and evaporation of the injected fuel exist in the free spray. These are the forward front and the dilute outer sleeve of the spray. In the high-velocity and dense axial flow core the heating is less intensive and evaporation of droplets is insignificant. After the impingement starts at first the evaporation rate of the fuel accumulated in forward front is sharply reduces in zone 4 in Fig. 8. It is caused by the lower (in comparison with the gas) temperature of the wall, by reduction in the rate of increase in diameters of droplets, by condensation of the droplets and of the gas mixture on the walls, by the combination and mixing of droplets at the front of the spray and of relatively colder droplets traveling behind when these also reach the wall surface. After spray front impinges the wall, a two-phase mixture starts to spread over the wall outside the boundaries of the cone 4 (Fig. 8) in the spray. The evaporation rate of the fuel located in the wall surface zone gradually increases, though this remains less than that in the chamber volume. To carry out numerical simulations of these processes the following assumptions are made to simplify the problem:

1) During the injection process the intensive heat exchange and evaporation take place in the zones of the dilute outer sleeve, the forward front and the NWF. Evaporation in the zone of the spray core is neglected.

2) The evaporation rate of the fuel in each zone of intensive heat exchange is equal to the sum of evaporation rates of individual droplets. The evaporation of each droplet prior and after ignition of the fuel is simulated by the Sreznevsky's equation:

$$d_k^2 = d_0^2 - K\, t_u \qquad (36)$$

where d_k is the current diameter of the droplet; d_0 is the initial diameter of the droplet; K is the constant of evaporation; t_u is the current time from the start of evaporation (from the instance when the droplet reaches the corresponding zone).

3) The fuel supply equipment of supercharged diesels provides relatively uniform atomization of fuel, especially during the basic phase of the injection process. Therefore the calculation of the evaporation rate of fuel can be carried out using the value of a mean Sauter droplet diameter d_{32}. It is assumed in calculations that $d_0 = d_{32}$.

4) The relationship, namely $K/d_0^2 = b_u$ during the injection period is used in each zone.

Effects of neglected factors and inaccuracies due to the above assumptions made will be then corrected using a special empirical correction function Y.

Equations for determination of the fuel evaporation rate ds_{ui}/dt in the i-zone was obtained by Razleytsev [6]:

$$ds_{ui}/dt = \left[1-\left(1-b_{ui}t_{ui}\right)^{3/2}\right] s_{zi}/t_{ui}\,; \qquad (37)$$

$$t_{ui} = t_s - t_{s0i} \qquad (38)$$

where t_{s0i} is the time of distribution of the fuel in the i–zone; s_{zi} is the fuel fraction in the i–zone. Constants of evaporation of fuel in various zones are determined as

$$K_{ui} = 4\cdot 10^6\, Nu_D\, D_p\, p_S / r_f \qquad (39)$$

where Nu_D is the Nusselt number for diffusion process; D_p is the diffusion factor for the fuel vapor under combustion chamber conditions; p_S is the pressure of the saturated fuel vapor; r_f is the density of liquid fuel. The diffusion factor is calculated using the following equation:

$$D_p = D_{po}\left(T_k/T_o\right)\left(p_o/p\right) \qquad (40)$$

Here D_{po} is the diffusion factor under atmospheric conditions [p_o, T_o], T_k is the equilibrium temperature of evaporation, p is the current pressure in the cylinder. Various conditions of evaporation in the different zones of the spray are taken into account by suitable values of T_k and Nu_D.

In the dilute outer zone there is a relatively large distance between fuel droplets and there is a small decrease in the temperature caused by the evaporation process. Therefore, in this zone it is assumed that Nu_D=2 [6]. During injection and combustion, the cylinder pressure and the temperature exceed critical levels for conversion of the liquid phase into the gaseous one. Therefore, in this zone the evaporation constant determined as $K_{env}=1.12\ 10^{-6}/p$, where the value of p is measured in MPa. In the case of the PCCI process Equations 39 and 40 are used to carry out relevant calculations.

In the forward front zone, the relatively cool droplets traveling in the spray core are rapidly heated, therefore in this zone $Nu_D \approx 20$ [6] and the temperature varies in the range between the critical value of 710 K and the fuel temperature. Thus in this zone the evaporation constant $K_{fr}=0.63\ 10^{-6}/p$. In the case of the PCCI process also Equations 39 and 40 are used for computations.

In the zones of the NWF, including zones located on the cylinder head and liner walls, the evaporation constants are calculated using equations 39 and 40 in which T_k is some effective temperature depending on the corresponding wall temperature T_{wi}:

$$T_k = \begin{Bmatrix} 550 & if & T_{wi} \le 400 \\ a\,T_{wi}^3 + b\,T_{wi}^2 + c\,T_{wi} + d & if & 400 < T_{wi} < 700 \\ 700 & if & 700 \le T_{wi} \end{Bmatrix};$$

Here a = 0.000000243; b = 0.001017919;

c = -0.854312919; d = 709.55496.

The Nusselt number for the NWF in Equation 39 depends on the surface shape: for the smooth surface of the combustion chamber Nu_D = 2; for the surfaces where the flow is turbulent Nu_D = 3 or higher [6]. A 16-year experience on the RK-model calibration using experimental data obtained over the whole operating range for various types of engines with the cylinder diameter ranging from 75 mm to 760 mm and with different combustion chambers and injector designs resulted in the following empirical correction function Y which takes into account the swirl ratio, the engine speed, the piston stroke and the Sauter mean diameter:

$$Y = 0.372 \cdot 10^{-9} \left(18 + y_S + y_{RPM}\right) y\, R_{S\,y}^{0.35}\, d_{32}^{-1.5} \qquad (41)$$

Here y_S=*f(S)* is the correction factor taking into account the effect of the piston stroke S, y_{RPM} =*f(RPM)* is the correction factor taking into account the effect of the engine speed, $R_{S\,y}$=*MAX(0.1, R_s)* is the corrected swirl ratio in the combustion chamber at TDC, $y \approx 35$ and is the correction factor derived from the RK-model calibrations using extensive experimental data from numerous tests. Factor y does not depend on the engine load and the speed. Considering the correction factor, the evaporation constant for the i-zone is $b_{ui} = Y\,K_i / d_{32}^2$. The fuel evaporation rate in each zone is calculated using Equation 37. The overall evaporation rate is found as a sum of the evaporation rates in all the m zones:

$$\frac{ds_u}{dt} = \sum_{i=1}^{m} ds_{ui}/dt \ . \qquad (42)$$

In the case of multiple injection the simulation of the spray evolution, the distribution of fuel in the corresponding zones and of evaporation of fuel is carried out for each stage of the multiple injection. The values of the characteristic gas temperature and the pressure for each portion of injected fuel from the previous cycle simulation are used in calculations.

HEAT RELEASE SIMULATION

For heat release simulation it is assumed that the heat release consists of four main phases. These phases differ from each other by physical and chemical processes and factors limiting the rate of these processes:

1. Induction period. In the case of the long induction period in the PCCI process the low temperature oxidation is possible;
2. Premixed combustion phase;
3. Mixing-controlled combustion phase;
4. Late combustion phase which follows the completion of the fuel injection.

When modelling the engine with a multiple injection process, the combustion of each injected portion is simulated separately taking into account the mass of the injected fuel and the air-fuel ratio corresponding to each portion.

PREDICTION OF AUTO-IGNITION DELAY PERIOD FOR HIGH TEMPERATURE COMBUSTION USING EMPIRICAL EQUATIONS

The auto-ignition delay period has to be predicted for each fuel portion during the multiple injection process. Fuel in the second (j =2), in the third (j =3) and following (j =4, 5, etc.) portions can be injected in the cycle after the instance corresponding to TDC with considerable delays and into domain containing a large fraction of burnt products. The application of classic equations for calculation of the auto-ignition delay period in such specific conditions does not provide correct results. The equation which provides a good agreement between numerical simulation results and experimental measurements for various types of engines has been derived in the present work on the basis of experimental data processing.

The auto-ignition delay period t_i for each j-portion of fuel was calculated using different methods for various engines running under different operational conditions and then the obtained results then were compared.

Method 1. Step-by-step calculation defines the ignition delay period from the Start Of Injection (SOI) until the Start Of Combustion (SOC):

$$SOC = \Theta - SOI + t_{iT}\left(p(\Theta), T(\Theta)\right) \cdot 6\,n \quad ; \qquad (43)$$

$$t_i = SOC - SOI$$

where Θ in deg. is the crank angle which is varied in small steps $\Delta\Theta$; p and T are the current cylinder pressure (MPa) and the temperature (K) as functions of crank angle Θ, respectively; n is the engine speed (RPM); t_{iT} (sec) is the ignition delay period determined from the modified Tolstov's equation [38]:

$$t_{iT} = 3.8 \cdot 10^{-6}\left(1 - 1.6 \cdot 10^{-4} n\right)\left(\frac{T}{p}\right)^m \exp\left(\frac{E_a}{8.312\,T}\right) C_C C_T \ ; (44)$$

Here C_T is the correction factor accounting for the temperature growth rate during the auto-ignition delay period; C_C is the correction factor accounting for the concentration of combustion products during the auto-ignition delay period; *m=MAX(0.5, (0.64 – 0.035 p))* and depends on the current cylinder pressure; E_a = 23000...28000 kJ/kmole is the activation energy in the auto-ignition process.

The correction factor C_T takes into account a gradient in the temperature change during the delay period which may be negative at the start of the injection process in the cycle after TDC. The late injection of fuel results in the increase of the ignition delay period. The value of the correction factor C_T was obtained from processing experimental data. Experimental data for the Caterpillar (D/S = 137/165 mm) diesel was published by Bakenhus and Reitz [39]; test data for the D49 (D/S = 260/260 mm) locomotive diesel with double injection was supplied by Kolomna locomotive diesels plant in Russia. The correction factor C_T is determined as:

$$C_T = 1, \qquad if\ x_t > 30;$$

$$C_T = -4 \cdot 10^{-7} x_t^3 + 5 \cdot 10^{-5} x_t^2 - 0.0032 x_t + 1.0832, \quad if\ x_t < 30;$$

$$x_t = \frac{T(\Theta) - T(\Theta - \Delta\Theta)}{1000\ \Delta\Theta} 6n;$$

where $T(\Theta)$ and $T(\Theta - \Delta\Theta)$ are measured in K and are the mean cylinder temperatures, Θ is the current CA and $\Delta\Theta$ is the change in CA. The dependence of C_T on x_t is shown in Fig. 11.

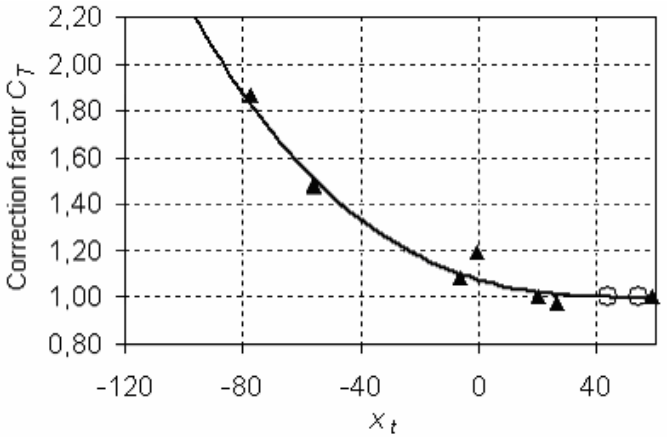

Figure 11. Correction factor C_T accounting for the temperature growth rate x_t in the auto-ignition delay period.
▲ - Bakenhus and Reitz data [39];
O – Kolomna plant data.

The correction factor C_C accounting for the composition of the air charge was also derived from processing experimental data. Experimental data published in [39-41] was obtained for both the engine conditions and in the bomb. Fig. 12 shows the dependence of the correction factor C_C on the composition of the gas into which fuel was been injected. The solid line presents a data approximation curve.

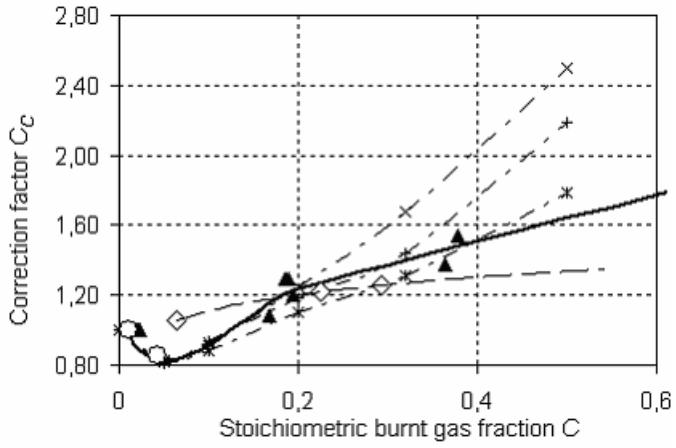

Figure 12. Correction factor C_C accounting for the stoichiometric burnt gas fraction during the auto-ignition delay period.
Engine conditions:
▲ - Bakenhus and Reitz [39];
◊ - Schneider, Stockli, Lutz, Eberle [41];
O – Kolomna plant;
Bomb conditions (Kwon, Arai, Hiroyasu [40])
Ú: T=700K, x : T=773 K, +: T=823K.

Both correction factors are equal to 1 for a conventional diesel with a small injection timing. However, the farther is the start of injection from TDC, the greater the correction factors will be. During multiple injection when the succession of the fuel portions are injected into the domain where there is the developed combustion process and the increased temperature, the correction factor C_T is close to 1 and the correction factor C_C has a dominant effect on the calculated auto-ignition delay period for the following fuel portion.

Comparison of the calculated ignition delay period (using the method described above) and published experimental data is shown in the Fig. 13. The calculated delays at the high values of SOI exceed values from experimental data. Table below shows the list of engines and their parameters used for plotting the diagram in Fig. 13.

Engine	D/S [mm]	RPM	BMEP [bar]	Source
DKRN 74/160	760/1600	120	9.5	*
VASA 6R46	460/580	500	22.7	[45]
		400	13.9	
		315	9.5	
D42	300/380	750	16	*
D49	260/260	1000	15.7	*
		845	11	
		563	3.3	
Cold start at -25C		350	0.16	
Experimental DI, PCCI	135/140	1000	0…2.4	[42, 43, 44]
KamAZ 7405	120/120	2200	12.2	*
		1800	13.8	
		1000	12	

* Data was presented by the engine manufacturer.

Analysis of presented data shows that the calculated values of the ignition delay exceed the measured ones.

Method 2. Integral calculation method [16] proposes the calculation of the t_i using the following relationship:

$$\int_0^{t_i} \frac{dt}{t_{iT}} = 1 \qquad (45)$$

where t_{iT} is calculated using Equation 44. The results obtained with this type of calculations are also shown in the Fig. 13. The values obtained are less than those from measured data at the high value of SOI.

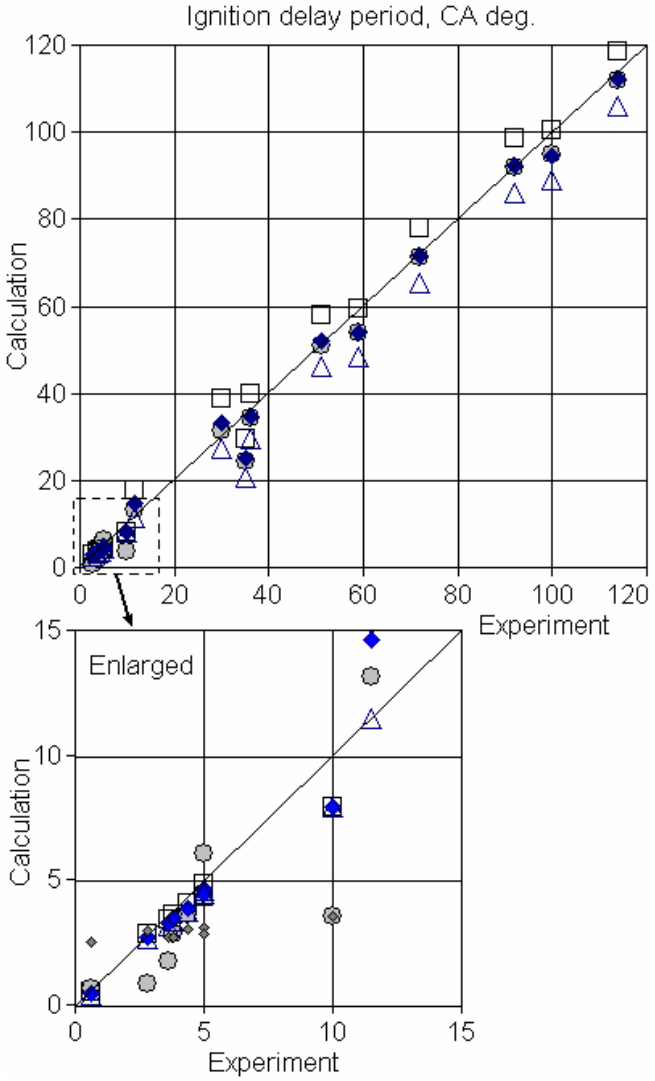

Figure 13. The comparison of the experimental ignition delays for different engines with the calculated ones obtained using different methods.
□ – Step-by-step calculation, Eq. 43 and 44;
Δ – Integral calculation, Eq. 45 and 44;
♦ – Average calculation, Eq. 43, 44, and 45;
● –Michigan University Equation [46];
♦ –Hardenberg and Hase Equation [47].

Method 3. Average calculation method uses the arithmetic average of the values from both previous methods. This method is in a very good agreement with the experiments over the whole range of the delay period variation, see Fig. 13.

Method 4. University of Michigan Equation. In this method [46] it is proposed to calculate the t_i as

$$\int_0^{t_i} \frac{dt}{t_{ign}} = 1;$$

$$t_{ign} = 1.3 \cdot 10^{-4} p^{-1.05} a^{-0.77} y_{O2}^{-1.41} \exp\left(\frac{33700}{RT}\right). \qquad (46)$$

where a is the air fuel ratio, y_{O2} is the concentration of oxygen, T and p are the current cylinder temperature (K) and pressure (atm). Results obtained using this method are also shown in the Fig. 13.

Method 5. Hardenberg and Hase Equation. The method [47] can not be used at the PCCI conditions because the application of the equation is restricted by the value of the maximum cylinder pressure, see Fig. 13.

Analysis of data presented in Fig. 13 shows that for engines with PCCI conditions the Average calculation method and University of Michigan equation provide the best accuracy. The Average calculation method is preferable for use in conventional conditions where the ignition delay is less than 10 CA deg. and for engines with the SOI in the cycle after TDC.

PREDICTION OF AUTO-IGNITION DELAY PERIOD USING DETAILED CHEMISTRY

The pressure and the temperature in the cylinder and the composition of the gas vary in a certain way during the ignition delay period and this is influenced by the way the working process is organized. For example there might be arrangements in the engine design for in-cylinder water injection or for implementation of the Z-Engine Concept [54] and in these cases the use of conventional methods for calculations of the ignition delay period will not provide satisfactory results. Furthermore, the empirical equations derived for the calculation of the ignition delay period in engines running on conventional diesel fuel could be proved to be inaccurate when the engine is switched to bio-fuel. In order to make calculations of the ignition delay period more universal the authors of this paper used the calculated 4D map of the ignition delay period as function of the temperature, the pressure, the equivalence ratio and the composition of combustion products in the cylinder. Such the 4-D map was created using CHEMKIN PRO software prior to the engine simulations. Mathematical modeling of kinetics of chemical reactions describing the process of ignition and combustion of the fuel at in-cylinder conditions is based on calculations of the speed of corresponding chemical reactions. The speed of chemical reaction is determined using the variation in the concentration (C) of each substance participating in the reaction. In general case any reaction can be presented as

$$\sum_{k=1}^{K} n'_{ki} C_k \Leftrightarrow \sum_{k=1}^{K} n''_{ki} C_k$$

where n_{ki} is stoichiometric coefficient of the k substance in the i -reaction; indexes ' and '' are used for direct and reversed reactions, respectively.

The speed of the change in the concentration of the k-substance is determined as

$$W_k = \sum_{i=1}^{I} n_{ki} w_i$$

where

$$n_{ki} = n''_{ki} - n'_{ki}$$

and w_i is the speed of the i-reaction:

$$w_i = k_{fi} \prod_{k=1}^{K} [x_k]^{n'_{ki}} - k_{ri} \prod_{k=1}^{K} [x_k]^{n''_{ki}}$$

Here x_k is the molar concentration of the k-substance; k_{fi} and k_{ri} are the speed constants of the direct and the reversed i-reaction, respectively. The speed constant for the direct reaction is determined using Arrhenius equation:

$$k_{fi} = A_i T^{b_i} \exp\left(\frac{-E_i}{RT}\right)$$

where A_i and b_i are constants for the i-reaction; T is the temperature; E_i the activation energy for the i-reaction; R is the gas constant.

The speed constant for the reverse reaction is calculated as $k_{ri} = \frac{k_{fi}}{K_{ci}}$,

where the equilibrium constant for the i-reaction

$$K_{ci} = \exp\left(\frac{\Delta S_i^0}{R} - \frac{\Delta H_i^0}{RT}\right) \cdot \left(\frac{p}{RT}\right)^{\sum_{k=1}^{K} n_{ki}}$$

Here ΔS_i^0 and ΔH_i^0 are the entropy and enthalpy changes following the full conversion of all the reactants into the products in the i-reaction, respectively; p is the pressure.

In parallel to calculations of the speed of chemical reactions and of the concentrations of substances the values of the temperature and pressure are determined in the corresponding volumes using the relevant relationships between thermodynamic properties [55].

The value of the ignition delay period t_{ign} is determined as the longest of the following two periods of time:

- The period of time ending in the instance corresponding to the maximum concentration of OH;
- The period of time ending in the instance when a sharp increase in the temperature in the volume starts (the maxim value of dT/dt is achieved with t being time);

For estimation of the period of the ignition delay in the diesel fuel a chemical mechanism of the combustion for n-heptane was used. Several chemical mechanisms for description of the combustion of n-heptane exist and in this work the following two mechanisms were considered:

- The reduced mechanism for rapid calculations by Reitz et al [56] which takes into account 52 reactions between 29 species;
- The extended mechanism developed at the Lawrence Livermore National Laboratory [57] which considers 1540 reactions between 160 species.

In this work the task was to investigate the influence of various combinations of the temperatures, the pressures and the composition of the air-fuel mixture over the wide range of these parameters. Therefore on the first stage of investigations the results obtained using the above two methods were compared against published experimental data [58, 59] for stoichiometric mixture of n-heptane with air. Fig. 14 presents results of the comparison of numerical results (shown in solid lines) with experimental data.

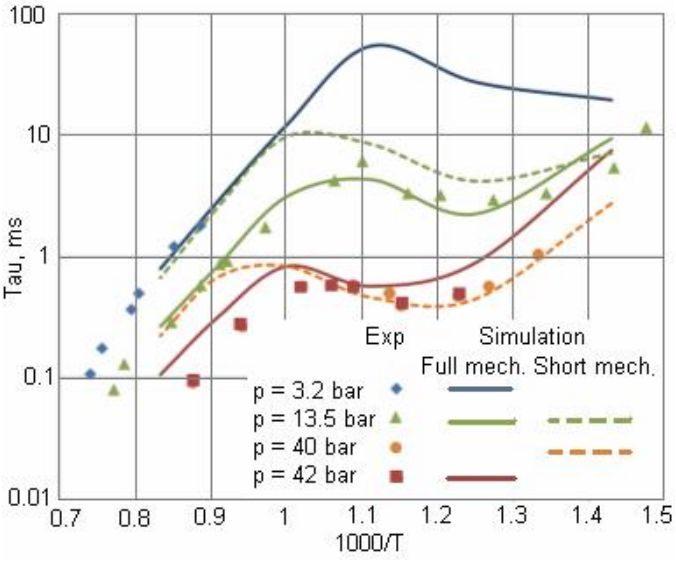

Figure 14. Numerical and experimental data on the value of the ignition delay period for n-heptane Numerical data was obtained using the reduced mechanism by Reitz R.D. et al [56] and the extended mechanism developed at the Lawrence Livermore National Laboratory [57].

It can be seen in Fig.14 that the reduced mechanism can be used for calculations of diesel engines with the conventional working cycle. If the ignition delay takes place at conditions in which there is a relatively low pressure (this is a specific feature of the PCCI and HCCI processes) then it is necessary to apply the extended mechanism developed at the Lawrence Livermore National Laboratory.

The further investigations of the extended chemical mechanism was carried out in order to determine the influence of individual reactions on the fuel ignition delay process. This was done by excluding the individual reactions from the chemical mechanism and by comparison the ignition delay periods for the mechanism including all reactions with that obtained in the mechanism with the excluded individual reaction. As a

result of such analysis the reactions were identified which provide the contribution to the change in the ignition delay period exceeding ±5%.

Fig. A1 in Appendix A shows some results of the above analysis. Calculations were performed at the temperature of 800 K and the pressure of 40 bar for the following compositions of the air-fuel mixture:

- For the stoichiometric mixture without the EGR;
- For the lean mixture (l = 0.2) without the EGR;
- For the stoichiometric mixture with the 30% EGR (C=0.3).

Results of calculations demonstrate that for all three above cases there are 24 reactions which have the most influence though the individual contributions of reactions vary depending on conditions during the ignition delay period, particularly as a function of the gravimetric air-fuel ratio. The conclusion can be drawn that for diesels with the conventional working cycle, and in which zones with the stoichiometric mixture always exist in the cylinder, calculations of the ignition delay period can be carried out using detailed kinetic analysis with equivalence ratio l =1. In engines with the PCCI process the fuel spray can reach such a condition that there are no zones with the stoichiometric air-fuel mixture in the cylinder and therefore the influence of the equivalence ratio must be taken into account along with the effects of the temperature, the pressure and the concentration of burnt gases.

Using extended chemical mechanism approach the 4D map was built for n-heptane containing the values of the ignition delay period for a wide range of the temperature, the pressure, the air/fuel ratio and the concentration of burnt gases corresponding to the in-cylinder conditions.

Figures A2, A3 and A4 in Appendix A present some results of these calculations of the ignition delay period. These diagrams were obtained by cutting the obtained 4D map by corresponding planes. The application of the extended chemical mechanism for the description of the ignition delay process allows us to considerably improve the accuracy of the determination of the start of the visible combustion in the cylinder of engines operating on prospective working cycles, particularly with PCCI/HCCI processes and with the induction of the fresh air-fuel mixture into cylinder which takes place simultaneously with the fuel injection or after the completion of the fuel injection (the latter is being implemented in the Z-Engine concept [55]).

PREDICTION OF AUTO-IGNITION DELAY PERIOD FOR LOW TEMPERATURE COMBUSTION

The Low Temperature Combustion (LTC) precedes the High Temperature Combustion (HTC) process. At present for simulation of the LTC and the HTC and for the prediction of the ignition delay period during these processes, the CHEMKIN code is mainly used and several researchers have reported that the LTC combustion starts in the narrow range of variation in the in-cylinder temperature, namely from 770 to 810 K. However, the use of CHEMKIN does not provide sufficiently accurate prediction of the LTC. In this investigation an attempt was made to predict the LTC ignition delay using the value of the HTC ignition delay which is computed in advance. Analysis of numerous published experimental and calculated data [42-44, 48-51] resulted in derivation of the expression for calculation of the LTC delay t_{iLTC} as a function of HTC delay t_{iHTC} and EGR ratio. Fig. 15 shows the dependence of the difference between HTC and LTC delays as a function of the HTC delay for various engines working at different speeds, BMEP, the air intake temperature, etc. The proposed equation for the calculation of the LTS delay is

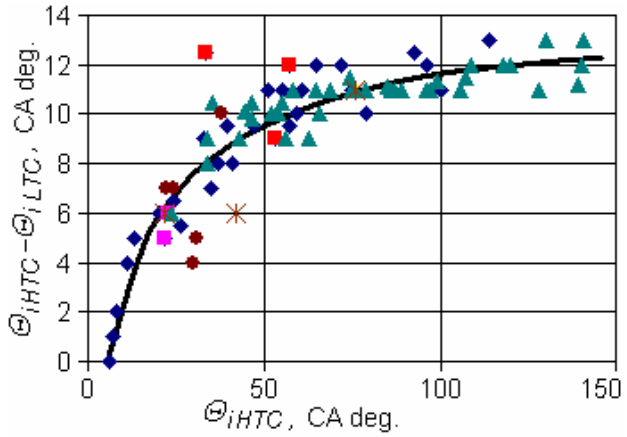

Figure 15. Difference between HTC and LTC delays as a function of the HTC delay period.

$$\Theta_{iLTC} = 8.281 + 1.0259\,\Theta_{iHTC} - 4.8822 \ln \Theta_{iHTC} - \sqrt{31.602\,C} \qquad (47)$$

where $\Theta_{iLTC} = t_{iLTC}\,6n$ and $\Theta_{iHTC} = t_{iHTC}\,6n$ are the LTC and the HTC delays in CA degrees, respectively; C is the EGR fraction.

HEAT RELEASE PREDICTION FOR LTC

The fraction of fuel burning in accordance with the low temperature mechanism can be calculated using the following proposed equation (also derived from processing data published in [42-44, 48-51]):

$$x_{LTC}^{\max} = (0.102 - 0.0392\,C) \cdot \left(\frac{81.6}{\exp \Theta} - \frac{8.88}{\Theta} + 1.2261 \right) \qquad (48)$$

where $\Theta = MAX\ (6.7,\ Q_{iLTC})$.

Heat release during the LTC can be approximated using the Wiebe expression, as a function of the crank angle j varied from the start of LTC:

$$x_{LTC}(j) = x_{LTC}^{\max}\left\{1-\exp\left[-2.9957\left(\frac{j}{j_z}\right)^{m_v+1}\right]\right\} \qquad (49)$$

where $m_v = 1.2+0.69\ C$ is the mode of Wiebe function; j_z = 6…8 CA deg and is the duration of the LTC.

HTC HEAT RELEASE PREDICTION

The fraction of fuel burning at the HTC is $x_{HTC}^{\max} = 1 - x_{LTC}^{\max}$.

The detailed description of equations obtained by Razleytsev for calculation of the heat release is presented in [6]. During the premixed combustion phase the heat release rate is:

$$dx/dt = f_0 P_0 + f_1 P_1 \qquad (50)$$

where $P_0 = A_0 (m_f/V_i)(s_{ud} - x_0)(0.1 s_{ud} + x_0)$;
$P_1 = ds_u/dt$.

During the mixing-controlled combustion phase, the heat release rate is:

$$dx/dt = f_1 P_1 + f_2 P_2 \qquad (51)$$

where $P_2 = A_2 (m_f/V_c)(s_u - x)(a - x)$.

After the fuel injection, during the late combustion phase the heat release rate is:

$$dx/dt = f_3 A_3 K_T (1-x)(x_b a - x). \qquad (52)$$

In the above equations it is assumed that $f_0 \approx f_1 \approx f_2 = f$ and is the function describing the completeness of the fuel vapor combustion in the zones:

$$f = 1 - \frac{A_1}{x_b a - x}\left\{r_V + \sum_{i=1}^{m_W}\left[300\, r_{Wi} \exp\left(\frac{-16000}{2500 + T_{Wi}}\right)\right]\right\}\frac{dx}{dt} \qquad (53)$$

where x_b is the efficiency of air use, α is the equivalence A/F ratio, r_V is the relative evaporation rate in the zones of the outer sleeve and the front, r_{Wi} is the relative evaporation rate in other NWF zones:

$$r_V = \frac{ds_{u\,env}/dt + ds_{u\,front}/dt}{ds_u/dt}, \quad r_{Wi} = \frac{ds_{u\,Wi}/dt}{ds_u/dt},$$

where m_W is the current number of zones formed by the NWF, T_{Wi} is the wall temperature of the corresponding zone. The efficiency of air use is described by the relation of the current equivalence A/F ratio in zones of combustion to the overall A/F ratio in the cylinder defined as a. On the basis of gas analysis performed for different diesel engines, the expression for x_b was obtained by Razleytsev in the following form:

$$x_b = 1 - 1.46\,(1 - x_{b0})\frac{\dot{j}_z}{\dot{j}_{z0}}\frac{2}{p}\exp\left[-\frac{1}{2}\left(\frac{\dot{j}_z}{\dot{j}_{z0}}\right)^2\right] \qquad (54)$$

where $\dot{j}_{z0}$=0.25...0.35 is a constant, $\dot{j}_z = j/j_z$ is the ratio of the current CA from the start of combustion (j) and the duration of the conventional combustion j_z, x_{b0} =0.35...0.45 for diesels with a compact piston bowl and x_{b0} =0.20...0.35 for medium and high speed diesels with an open combustion chamber (Hesselman). The duration of the conventional combustion is determined by the evaporation period of large droplets injected at the end of the injection process:

$$j_z = (t_{inj} - t_i + t_{l\,burn})6n; \qquad (55)$$

$$t_{i\,burn} = d_l^2/K_u\left[1 + 2.5\cdot 10^6\, K_O/(a-1)\right]; \; K_u = Y K_O$$

where d_l is the diameter of the largest droplet. In Equations 50-55 the following notations are used: m_f is the fuel mass in the current and the previously injected portions, V_i and V_c is the cylinder volume at the beginning of the HTC of the current portion of fuel and at TDC, respectively; s_{ud} and s_u are the fuel fractions evaporated by the current moment of time and during the ignition delay period, respectively; A_0, A_1, A_2 are empirical factors depending on the engine speed and the swirl intensity and A_3 can be determined using Equations 51 and 52 at $t = t_{s\,max}$. From extensive experience of the RK-model calibration for various engines the following relationships are proposed in this paper:

$$A_0 = a_0 (R_S\, n)^{0.5};\; A_1 = 0.04/(R_S\, n)^{0.5};\; A_2 = 9(R_S\, n)^{0.5}. \qquad (56)$$

Parameter K_T takes into account the effect of the destruction of the NWF located on the piston crown due to the piston acceleration and is related to the phenomenon taking place in the narrow clearance between the piston and the cylinder head:

$$K_T = \begin{cases} 1, & if\ Z < Z_n \\ 1 + 3000\, s_{crown}(Z^2 - Z_n^2), & if\ Z \ge Z_n \end{cases}; \qquad (57)$$

$$Z = (dV/dj)/V$$

where V is the current cylinder volume, j is the CA, Z_n is the value of Z at 15° after TDC. The presented combustion model allows us to predict the heat release in the cylinder without recalibration for other operating modes.

The RK-model was implemented into full-cycle thermodynamic engine simulation software DIESEL-RK described in [52]. The software can be installed on conventional PCs with Windows XP/Vista/7 operating systems. The calculation time depends on the number of differently orientated sprayer nozzles and the strategy of multiple injection, but it is usually takes under one minute to complete calculations with all iterative procedures.

RESULTS OF HEAT RELEASE SIMULATION FOR ENGINE WITH PCCI

Validation of the above diesel combustion model was performed using the following engines to confirm the capability of the RK-model to simulate working processes with high accuracy: the conventional diesel running over the whole operating range [53]; diesel fuel combustion and NO emission formation in the engine with a multiple injection [1], combustion in a two stroke engine with a side injection system [36] and to simulate diesel combustion with the PCCI process. The ability of the combustion model to accurately simulate the effects of multiple injections and EGR is also very important. A key characteristic of this computer code is its ability to carry out computer optimization of the engine control algorithm at any operating mode. The computer optimization is necessary to reduce high cost experimental investigations due to a considerable number of variable parameters which may be controlled to reduce emissions and SFC simultaneously. There are few ways to search for an optimal solution: by using the built in DIESEL-RK software library of non-linear optimization procedures [2] or apply external optimization software. To be used with external optimization software the DIESEL-RK code is equipped with a special interface for data exchange in the format of text files.

Fig. 16 and 17 show the computational results obtained on the mixture formation and combustion in the Peugeot DW10-ATED4 diesel (4L, S/D=85/88 mm) with a Common Rail injection system.

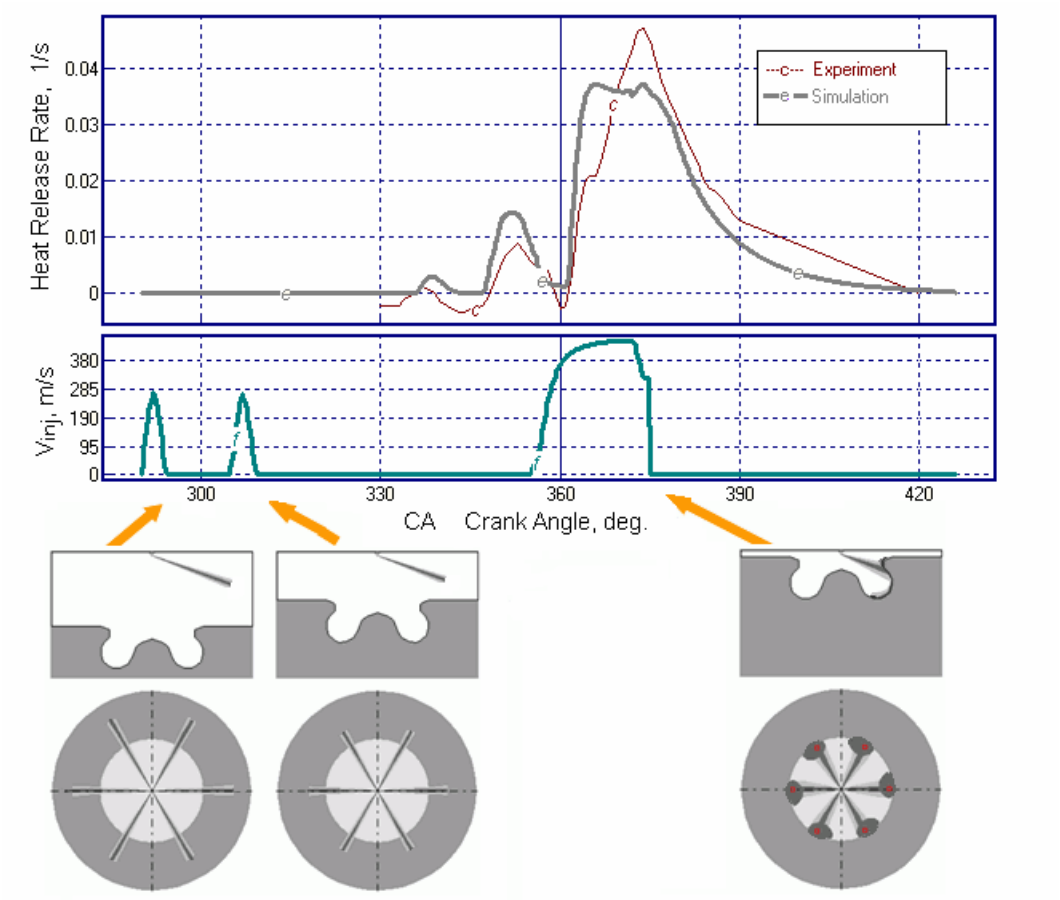

Figure 16. Computational results on the mixture formation and combustion in the Peugeot DW10-ATED4 diesel. The fraction of the total pilot injection is 0.15.

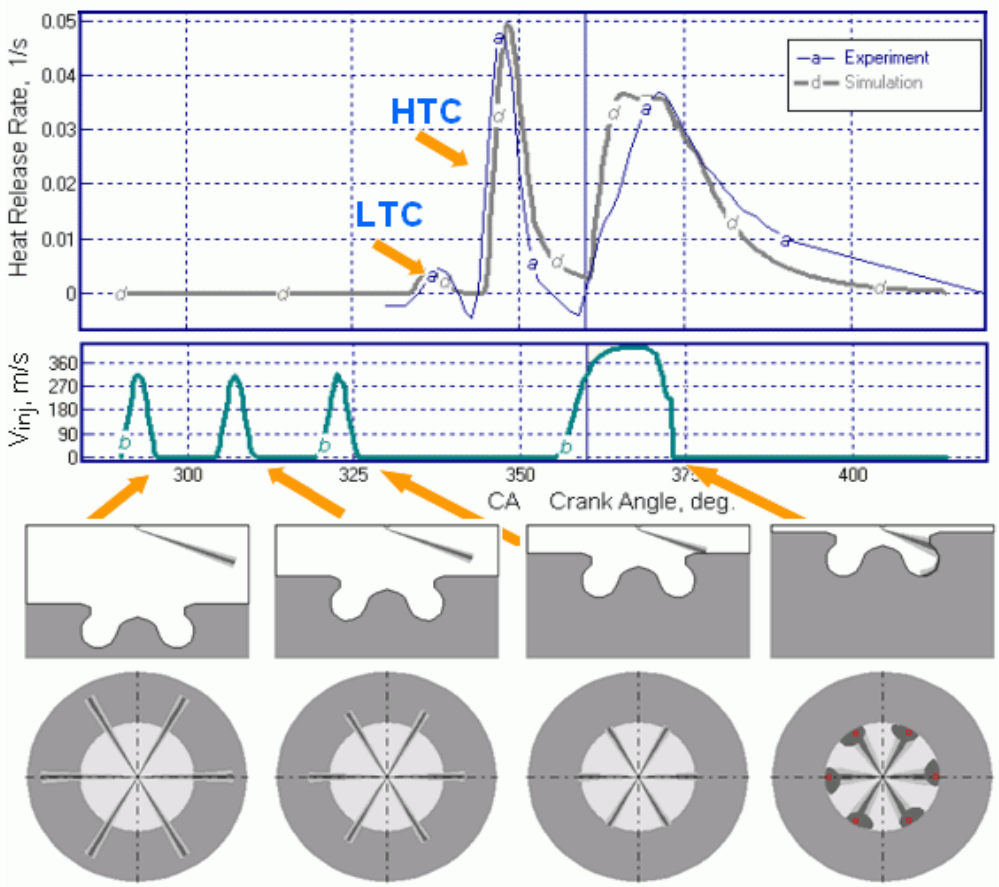

Figure 17. Computational results on the mixture formation and combustion in the Peugeot DW10-ATED4 diesel. The fraction of the total pilots injections is 0.35.

Experimental data for this engine was presented in [48]. In both cases the BMEP is 7.58 bar at the engine speed of 2600 RPM, the EGR is 9.8%. The total pilot injection fractions are 0.15 and 0.35 in the Fig. 16 and 17, respectively. In both cases the PCCI was arranged by implementing multiple pilot injections with the injection timing equal to 70 deg. before TDC. The duration of each pilot injection was set to be short in order to prevent the impingement of fuel on the cylinder liner. The injection profiles shown in Fig. 16 and 17 and the experimental heat release curves were taken from [48]. Frames below diagrams show the position of the sprays at the end of every injected portion. The first heat release peaks correspond to the LTC taking place prior the HTC.

Fig. 18 and 19 presents results of numerical calculations on the variation of gas parameters during the process of compression. Analysis of these results shows that all three portions of the fuel pilot injections are ignited practically simultaneously, see Fig. 19. This is indicated by coincidence of the curves of the integral function

$$\int_0^{t_i} \frac{dt}{t_{ign}} \qquad (58)$$

which is calculated for each portion of injected fuel. In general the difference in injection timing of these three portions of fuel should result in that the growth rate of the integral function for the earlier injected fuel portion should exceed that for following pilot fuel injections. However this does not happen since the long ignition delay at the relatively low pressure and temperature has a very little effect in the process of integration in Equation 58. Furthermore, as spray disintegrates in the time and large fuel droplets evaporate then the air/fuel ratio for earlier injected fuel portions rises and this results in the increase of the ignition delay period and in the slowing of the growth rate of integral function (58).

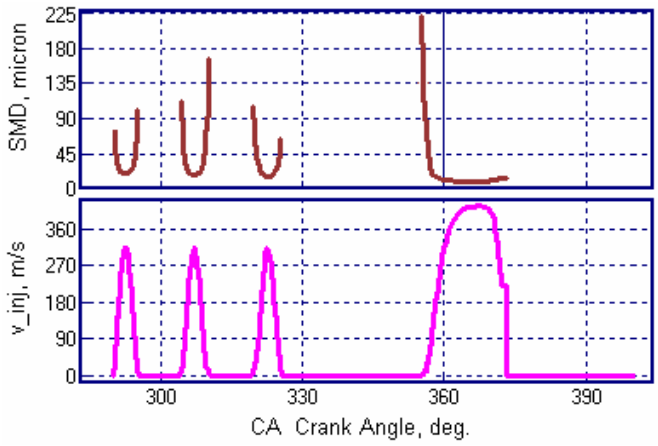

Figure 18. Variation of Sauter mean diameter of the fuel droplets for different portions of injected fuel. The fraction of the total pilot injections is 0.35.

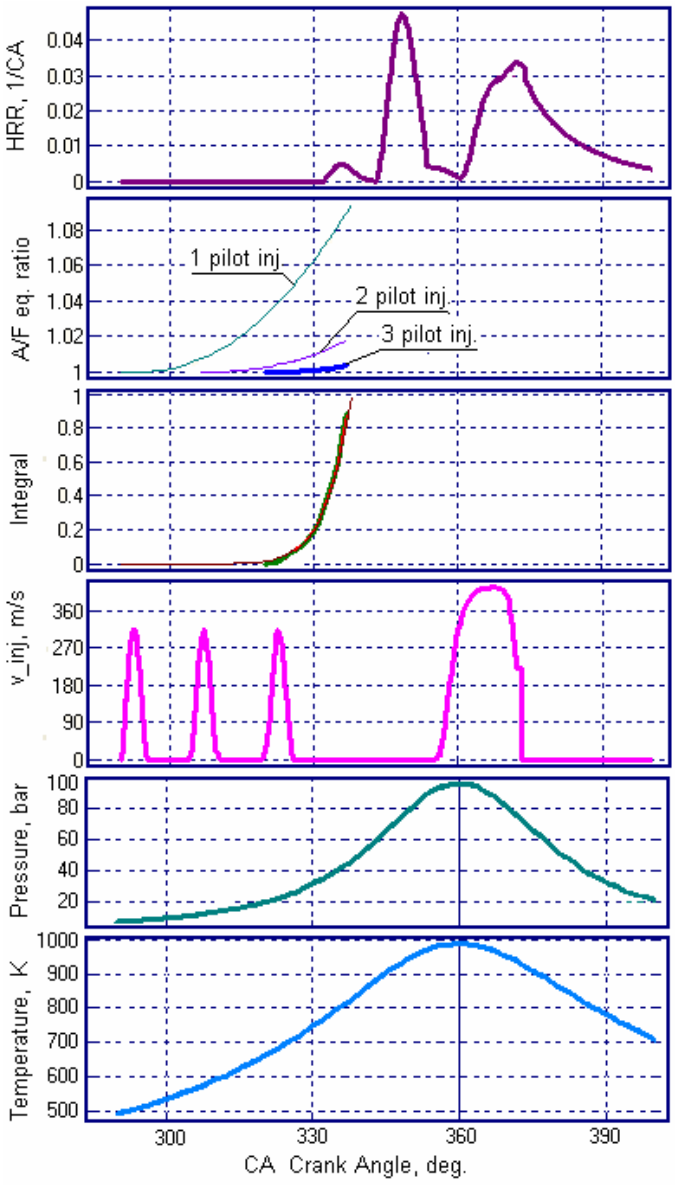

Figure 19. Variation of in-cylinder parameters for the Peugeot DW10-ATED4 diesel. The fraction of the total pilots injection is 0.35.

In determination of the air-fuel ratio, which is then used for calculation of the ignition delay for each portion of the pilot injection, the mass of the previously injected portion of fuel is taken into account. The period of evaporation of large droplets of fuel supplied into the cylinder in the last stages of the injection process is calculated using Equation 36.

The application of the proposed method of calculation of the ignition delay period and the heat release rate makes it possible to analyse the PCCI processes with the relatively higher values of the advancement in the fuel injection and in which the last portion of fuel injected at the instance of time when the piston is close to the TDC position is used for initiation of ignition of the lean mixture which otherwise would not ignite since $\alpha = 1 / l > 1$.

CONCLUSIONS

The presented RK-model is intended for diesel combustion simulation and it takes into account and optimizes the piston bowl shape, the injector design and its location, the shape of the injection profile including multiple injection modes. The RK-model also accounts for the droplet sizes, interaction of free fuel sprays with the swirl, the spray/wall impingement, the evolution of the near-wall flow formed by the spray, fuel reaching the surfaces of the cylinder head and of the cylinder liner, mixing of the NWF formed by adjacent sprays, the effect of the piston motion and of the swirl intensity on the heat release rate. The multi-zone RK-model takes into account the EGR, temperatures of the piston and the cylinder head in calculations of the heat release process. The model has capability to accurately predict the heat release rate, NOx and smoke emissions for different diesels working over the whole operating range without necessity for recalibration. The ability to predict diesel parameters with high accuracy for different kinds of injection profiles including multiple injection with long injection timing (PCCI), makes it possible to use this model for development of the Common Rail system controlling algorithm. As mentioned above the RK-model makes it possible to design the piston bowl shape and select the number, the diameter and orientation of injector holes to match the swirl intensity and this is used for controlling emissions and the fuel consumption. The RK-model includes Detailed Kinetic Mechanism for both prompt and thermal NOx formation simulations.

The RK-model can be used on conventional desktop and laptop PCs with running time of several seconds (the computational time of the diesel with two stage injection is about 10-12 seconds) and therefore it can be coupled with optimization software to search for the optimal combination of engine parameters to provide low levels of emissions and of the SFC.

The application of multi-parametric optimization procedures in combination with the RK-model of engines provides the high efficiency of computational research which is very important in engine design process.

ACKNOWLEDGMENTS

The authors gratefully acknowledge contribution and support of academic staff at the BMSTU, in particular of Professor Nikolay Ivaschenko. The authors also would like to thank Mr. Yuriy Fadeyev for his work on the development of the DIESEL-RK computer code.

REFERENCES

1. Kuleshov, A.S. Use of Multi-Zone DI Diesel Spray Combustion Model for Simulation and Optimization of Performance and Emissions of Engines with Multiple Injection. 2006, SAE Paper No 2006-01-1385.
2. Kuleshov, A.S. Multi-Zone DI Diesel Spray Combustion Model and its application for Matching

the Injector Design with Piston Bowl Shape. 2007, SAE Paper No 2007-01-1908.
3. A. Kuleshov and K. Mahkamov. Multi-zone diesel fuel spray combustion model for the simulation of a diesel engine running on biofuel. Proceedings Of IMECHE, Part A, Journal of Power and Energy. 2008. pp. **222**, 309 – 321.
4. Zeldovich Ya.B., Raizer Yu.P.: "Physics of shock waves and high-temperature hydrodynamic phenomena", Moscow: Nauka, 686 p., 1966. (In Russian).
5. Zvonov V.A.: "Internal combustion engines toxicity", Moscow: Mashinostroenie, 200 p., 1973. (In Russian).
6. Razleytsev N.F.: "Combustion simulation and optimization in diesels", Kharkov: Vischa shkola, 169 p., 1980. (In Russian).
7. Miller J.A., Bowman C.T. Mechanism and modeling of nitride. Chemistry in Combustion // Prog. Energy Combustion Science. – 1989. – v.15. – P.287-338.
8. Bochkov M.V., Lovachev L.A., Hvisevich S.N. Formation of the Nitrogen Ox-ide (NO) at Laminar Flame Propagation in the Homogeneous Air-Methane Mixture // FGV – vol. 34 – 1998. – No 1. (in Russian).
9. Bochkov M.V., Lovachev L.A., Hvisevich S.N. Numerical Modeling the NOx Formation at Air-Methane Mixture Combustion at Condition of Coupled Processes of Chemistry Kinetic and Molecules Diffusion // Mathematical Modeling. – 1997. – No3. – vol. 9. – pp. 13-28. (in Russian).
10. Kamimoto, T., Kobayashi, H., and Matsuoka, S.: "A Big Size Rapid Compression Machine for Fundamental Studies of Diesel Combustion", SAE Paper 811004, SAE Trans., vol. 90, 1981.
11. Reitz, R.D. and Bracco, F.V.: "On the dependence of Spray Angle and Other Spray Parameters on Nozzle Design and Operating Conditions", SAE paper 790494, 1979.
12. Bracco, F.V.: "Modeling of Engine Sprays", SAE Paper No 850394, 1985.
13. Kuo, T.W. and Bracco, F.V.: "Computations of Drop Sizes in Pulsating Sprays and of Liquid-Core Length in Vaporizing Sprays", SAE Paper No 820133, SAE Trans., vol. 91, 1982.
14. Kaluzhin S.A., Romanov S.A., Sviridov Yu.B.: "Experimental investigation into velocities of liquid and gaseous phases in diesel fuel flame", Dvigatelestroenie, No. 7, pp. 5-8, 1980. (In Russian).
15. Lyn, W.T.: "Study of Burning Rate and Nature of Combustion in Diesel Engines", in Proceedings of Ninth International Symposium on Combustion, pp. 1069-1082, The Combustion Institute, 1962.
16. Heywood, J.B.: Internal Combustion Engine Fundamentals, McGraw-Hill, New York, 1988.
17. Dragunov G.D., Egorov V.V.: "Some peculiarities of fuel moving along the combustion chamber surface", Izv. Vuzov, Mashinostroenie, No. 1, pp. 119-122, 1977. (In Russian).
18. Egorov V.V.: "Investigation into peculiarities of fuel evaporation and working cycle in boosting the tractor diesel with the CNIDI combustion chamber", Ph. D. Thesis, Leningrad, 1978. (In Russian).
19. Ivanchenko N.N., Semenov B.N., Sokolov V.S.: "Working process in diesels with piston bowl", Leningrad, Mashinostroenie, 228 p., 1972. (In Russian).
20. Novoselov V.D.: "Investigation into working process of four-stroke diesels based on ChN26/26 engines with mean effective pressure above 20 kg/cm^2 with limitations on maximum combustion pressure", Ph. D. Thesis, Leningrad, 1978. (In Russian).
21. Semenov B.N.: "Theoretical and experimental fundamentals of applying fuels with various physical and chemical properties in high-speed diesels", Dr. Snc. Thesis, Leningrad, 1978. (In Russian).
22. Sokolov S.S., Demidova N.I., Safonov V.K.: "Increase of diesel reliability by optimization of combustion chamber", Energomashinostroenie, No. 2, pp. 12-14, 1973. (In Russian).
23. Semenov B.N., Pavlov E.P.: "Investigation and development of volume and film fuel-air mixing in diesels", Energomashinostroenie, No. 1, pp. 7-10, 1978. (In Russian).
24. Balles, E.: "Fuel-Air Mixing and Diesel Combustion in a rapid Compression Machine", Ph.D. Thesis, Department of Mechanical Engineering, MIT, June 1987.
25. Gavrilov V.V.: "Methods increasing quality of fuel-air mixing and combustion in a marine diesel based on mathematical and physical simulation of local intracylinder processes", Dr. Snc. Thesis, Saint Petersburg, StPb SMTU, 2004. (In Russian).
26. Lyshevsky A.S.: "Fuel atomization in marine diesels", Leningrad, 248 p., 1971. (In Russian).
27. Kuo, T.W., and Bracco, F.V.: "On the Scaling of Transient Laminar, Turbulent and Spray Jets", SAE Paper No. 820038, 1982.
28. Hiroyasu, H., Kadota, T and Arai, M.: "Supplementary Comments: Fuel Spray Characterization in Diesel Engines", Combustion Modeling in Reciprocating Engines, Ed. By Mattavi, J.N. and Amann, C.A., pp. 369 – 408, Plenum Press, N.Y., 1980.
29. Arregle, J., Pastor, J.V. and Ruiz, S. The Influence of Injection Parameters on Diesel Spray Characteristics. 1999, SAE Paper No. 1999-01-0200, 1999.
30. Pastor, J.V., Encabo, E. and Ruiz, S. New Modelling Approach for Fast Online Calculations In Sprays. 2000, SAE Paper No. 2000-01-0287.
31. Larmi, M., Rantanen, P., Tiainen, J., Kiijarvi, J., Tanner, F.X. and Stalsberg-Zarling, K. Simulation of Non-Evaporating Diesel Sprays and Verification with Experimental Data. 2002, SAE Paper No. 2002-01-0946.
32. Nakagawa, H., Oda, Y., Kato, S., Nakashima, M and Tateishi, M. Fuel Spray Motion in Side Injection Combustion System for Diesel Engines. Proceedings of the International Symposium COMODIA 90, 1990, 281-286.

33. Reitz, R. D. and Bracco, F. B. On the Dependence of Spray Angle and Other Spray Parameters on Nozzle Design and Operating Conditions // SAE Paper 790494, 1979.
34. Dan T. The Turbulent Mechanism and Structure of Diesel Spray. Ph. D. Thesis, Toshisya University, 1996.
35. A.S. Kuleshov: "Multi-Zone DI Diesel Spray Combustion Model for Thermodynamic Simulation of Engine with PCCI and High EGR Level", SAE Paper No 2009-01-1956, 2009.
36. A.S. Kuleshov: "Multi-Zone DI Diesel Spray Combustion Model and its application for Matching the Injector Design with Piston Bowl Shape", SAE Paper No 2007-01-1908, 2007.
37. Sviridov Yu.B., Malyavsky L.V., Vihert M.M.: “Fuel and fuel supply in automotive diesels”, Leningrad, 224 p., 1972. (In Russian).
38. Tolstov A.I. Indicated period of ignition lag and dynamic of cycle of high speed engine with compression ignition. // Tr. NILD "Research of working cycle and fuel supply in the high speed diesels". N1. M.: Mashgiz, 1955. pp. 5-55. (In Russian).
39. Marco Bakenhus and Rolf D. Reitz: “Two-Color Combustion Visualization of Single and Split Injections in a Single-Cylinder Heavy-Duty D.I. Diesel Engine Using an Endoscope-Based Imaging System”, SAE Paper No. 1999-01-1112, 1999.
40. Soon-Ik Kwon, Masataka Arai, Hiroyuki Hiroyasu: “Ignition Delay of a Diesel Spray Injected Into a Residual Gas Mixture”, SAE Paper No. 911841, 1991.
41. Schneider W., Stockli M., Lutz T., Eberle M. Hochdruckeinspritzung und Abgasrezirkulation im kleinen, schnellaufenden Dieselmotor mit direkter Einspritzung. MTZ. N 11, 1993. S.588-599.
42. Hisashi Akagawa, Takeshi Miyamoto, Akira Harada, Satoru Sasaki, Naoki Shimazaki, Takeshi Hashizume, Kinji Tsujimura "Approaches to solve problems of the premixed lean diesel combustion". SAE Pap No 1999-01-0183, 1999, 13 p.
43. Akira Harada, Naoki Shimazaki, Satoru Sasaki, Takeshi Miyamoto, Hisashi Akagawa and Kinji Tsujimura "The Effect of Mixture Formation on Premixed Lean Diesel Combustion Engine". SAE Pap No 980533, 1998, 10 p.
44. Yoshiaki Nishijima, Yasuo Asaumi, Yuzo Aoyagi "Premixed lean diesel combustion (PREDIC) using impingement spray system". Sae Pap No 2001-01-1892, 2001, 9 p.
45. Wartsila. Technology review: (http://www.wartsila.com/Wartsila/global/docs/en/ship_power/media_publications/brochures/product/engines/w46_tr.pdf)
46. X. He, M.T. Donovan, B.T. Zigler, T.R. Palmer, S.M. Walton, M.S. Wooldridge, A. Atreya "An Experimental and modeling study of iso-octane ignition delay times under homogeneous charge compression ignition conditions" // Combustion and Flame, 142 (2005) 266-275.
47. Hardenberg H.O. and Hase F.W. Empirical Formula for Computing the Pressure Rise Delay of a Fuel from its Cetane Number and from the Relevant Parameters of Direct-Injection Diesel Engines // SAE Paper 790493, 1979.
48. Gary D. Neely, Shizuo Sasaki, Jeffrey A. Leet "Experimental investigation of PCCI-DI combustion on emissions in a light-duty diesel engine", SAE Pap No 2004-01-0121, 2004, 11 p.
49. Kazuhisa Inagaki, Takayuki Fuyuto, Kazuaki Nishikawa, Kiyomi Nakakita, Ichiro Sakata "Combustion System with Premixture-controlled Compression Ignition". Research Report R&D Review of Toyota CRDL Vol. 41, No 3, 2006, pp 35-46.
50. Wanhua Su, Tiejian Lin, Yiqiang Pei "A compound technology for HCCI combustion in a DI diesel engine based on the multi-pulse injection and the BUMP combustion chamber". SAE Pap No 2003-01-0741, 2003, 10 p.
51. Ryo Hasegawa, Hiromichi Yanagihara "HCCI combustion in DI diesel engine" SAE Pap No 2003-01-0745, 2003, 8 p.
52. http://www.diesel-rk.bmstu.ru
53. A.S. Kuleshov: “Model for predicting air-fuel mixing, combustion and emissions in DI diesel engines over whole operating range”, SAE Paper No 2005-01-2119, 2005.
54. http://www.aumet.fi/html/z_engine.htm
55. Isaev, S.I. Textbook of Chemical Thermodynamics, High School publishing house, Moscow, 1986, 272 pages. (In Russian).
56. Ra, Y.,Reitz, R.D. A Reduced Chemical Kinetic Model for IC Engine Combustion Simulations with Primary Reference Fuels // Combust. Flame, Vol. 155, pp. 713–738, 2008.
57. https://www-pls.llnl.gov/?url=science_and_technology-chemistry-combustion-mechanisms
58. Seiser H., Pitsch H., Seshadri K., Pitz W.J., and Curran, H. J., Extinction and Autoignition of n-Heptane in Counterflow Configuration, Proceedings of the Combustion Institute, Volume 28, p. 2029-2037, 2000.
59. Liang L., Reitz R.D., Iyer C.O.,Yi J. Modeling Knock in Spark-Ignition Engines Using a G-equation Combustion Model Incorporating Detailed Chemical Kinetics. SAE paper. No 2007-01-0165, 2007.

CONTACT

Dr. Andrey Kuleshov,
Piston Engine Department of Bauman Moscow State Technical University,
2-Baumanskaya, 5, 105005, Moscow, Russia,
Tel.: +7(499) 265-78-92
e-mail: kuleshov@power.bmstu.ru
http://www.diesel-rk.bmstu.ru

ABBREVIATIONS

CA: Crank angle.

CFD: Computational Fluid Dynamic

DI: Direct Injection.

DKM: Detailed Kinetic Mechanism

EFM: Elementary Fuel Mass injected during one time step increment.

EGR: Exhaust Gas Recirculation.

FSV: Fuel Spray Visualization.

HCCI: Homogeneous Charge Compression Ignition.

HTC: High Temperature Combustion.

LTC: Low Temperature Combustion.

NWF: Near Wall Flow.

PCCI: Premixed Charge Compression Ignition.

PM: Particulate Matter emission.

SFC: Specific Fuel Consumption.

SOC: Start of combustion (CA deg. before TDC).

SOI: Start of injection (CA deg. before TDC).

NOMENCLATURE

b_{ui} : Evaporation constant for the i-zone.

b_m : Depth of the spray forward front, m.

C : the EGR fraction in the cylinder.

C_C: The correction factor accounting for the composition of the air charge.

C_T : The correction factor accounting for the temperature growth rate in the auto-ignition delay period.

d_{32} : Sauter mean diameter, m.

D_{po}: The diffusion factor of fuel under the atmospheric conditions, s.

D_p : The diffusion factor for the fuel vapor under the combustion chamber conditions, s.

d_k : The current diameter of the droplet, m.

d_l : the diameter of large droplets of fuel, m.

d_n : The nozzle hole diameter, m.

d_0 : The initial diameter of the droplet; m.

dx/dj : The heat release rate, 1/deg.

dx/dt: The heat release rate, 1/sec.

dt : the time step, sec.

dQ : the time step for the autoignition calculation, CA deg.

dj : the time step, CA deg.

h_{clr} : The piston-head clearance depending on CA, m.

l_{wj} : Dimensions of the NWF formation in each direction, m.

K_i : The theoretical evaporation constant in the i-zone.

K_j : Factor of the form of the NWF.

l : The current distance between the injector's nozzle and the EFM, m.

l_m : the EFM's penetration distance, m.

M : The squared Ohenzorge number.

m_f : The cycle fuel mass.

n : The engine speed [RPM].

Nu_D : The Nusselt number for diffusion process.

p_S : The pressure of the saturated fuel vapor.

r_f : The density of liquid fuel, kg/m^3

P_{inj} : The injection pressure.

$P_{inj\,max}$: The maximum injection pressure.

p : The pressure in the cylinder.

S : The piston stroke, m.

T_k : The effective temperature of the zone inside the NWF depending on the corresponding wall temperature, K.

U : The current velocity of the EFM, m/s.

U_o : The initial velocity of the EFM at the nozzle of the injector, m/s.

T_{wi} : The wall temperature, K.

V_{inj} : The injection velocity, m/s.

V : In-cylinder volume, Zone volume, m^3.

V_i : The cylinder volume at the beginning of the HTC of the current fuel portion m^3.

V_c : The cylinder volume at TDC, m^3.

p : The in-cylinder pressure.

R_s : The swirl ratio.

R : The cylinder radius, m.

r_V: The relative evaporation rate in the zones of the outer sleeve and of the front.

r_{Wi} : The relative evaporation rate in the different NWF zones.

T : The temperature, K.

T_{Wi} : The wall temperature of a corresponding zone, K.

U : The current velocity of EFM, m/s.

U_{0m} : The average injection velocity, m/s.

U_t : The tangential velocity of EFM in the swirl direction, m/s.

We : Weber number.

W_t : The local tangential air velocity, m/s.

x : The fraction of burnt fuel.

x_t : The temperature growth rate at the auto-ignition delay period, K/sec.

Y : The empirical correction function.

y_S : The correction factor depending on the piston stroke.

y_{RPM} : The correction factor taking into account the engine speed.

y_{O2} : The concentration of oxygen in the equation of the Michigan University for the self ignition delay.

a : the A/F equivalence ratio in the cylinder.

g : The spray angle, rad.

g_j : The impingement angles, rad.

x_b : The efficiency of in-cylinder air use.

f : The function describing the completeness of the fuel vapor combustion in the zones.

f : The Air-fuel ratio in the equation of the Michigan University for the self ignition delay.

j : The Crank Angle used at the combustion simulation.

j_z : The combustion duration in CA deg.

l : The Fuel / Air equivalence ratio.

m_f : The dynamic viscosity of fuel, Pa s.

r : The dimensionless density.

r_{air} : The air density, kg/m^3.

r_f : The fuel density, kg/m^3.

t : Time, sec.

t_s : The current time from the start of the injection, s.

$t_{s\,max}$: The time of the spray evolution, sec.

t_i : The auto-ignition delay period, sec.

t_{inj} : Injection duration, sec.

t_k : Travel time for the EFM to reach a distance l from the injector's nozzle, s.

t_m : Travel time for the EFM to reach a distance l_m from the injector's nozzle, s.

t_{sw} : Time for the spray to reach the wall, s.

t_w : Time of evolution of the NWF along the wall, s.

t_{s0i} : Time of arrival of fuel into the *i*–zone, s.

t_{iT} : The auto-ignition delay period calculated as a function of the current pressure and temperature, sec.

t_{ign} : The auto-ignition delay period calculated as a function of the current pressure, the temperature and the composition, sec.

t_u : The current time from the start of evaporation, s.

t_{lburn} : The time of evaporation and combustion of large droplets of fuel, sec.

Θ: The Crank Angle used for the ignition delay calculations.

Θ_i : The auto-ignition delay period, CA deg.

s : The fraction of fuel.

s_f : The fuel surface density, N/m.

s_u : The fraction of fuel evaporated by the current moment of time.

s_{ud} : The fraction of fuel evaporated during ithe gnition delay period.

s_{ui} : The fraction of fuel evaporated by the current moment of time in the i-zone.

s_{zi} : The fuel fraction in the *i*–zone.

ν : the air kinematical viscosity, m^2/s.

χ : The swirl damping factor.

ω : The angular velocity of the swirl, rad/s.

ω_C : The angular velocity of the crank, rad/s.

Э : The dimensionless parameter.

SUBINDEXES

air : Air

a : Initial domain of the spray forming.

b : Main domain of the spray evolution.

core : Dense core of the free spray.

crown : Crown of the piston.

cross : Zones of the NWF mixing.

env : The dilute outer sleeve.

f : Fuel.

front : The forward front of the free spray.

head : The cylinder head.

g : The boundary between the initial and main domains of the spray forming during the spray evolution.

j : The direction indexes;

liner : The cylinder liner.

k : The control section.

m : the section located behind the forward front.

s : The spray tip section.

w : The near wall flow.

w env : The dilute outer surrounding of the NWF.

w fr : The forward front of the NWF.

w core : The dense core of the NWF.

APPENDIX A

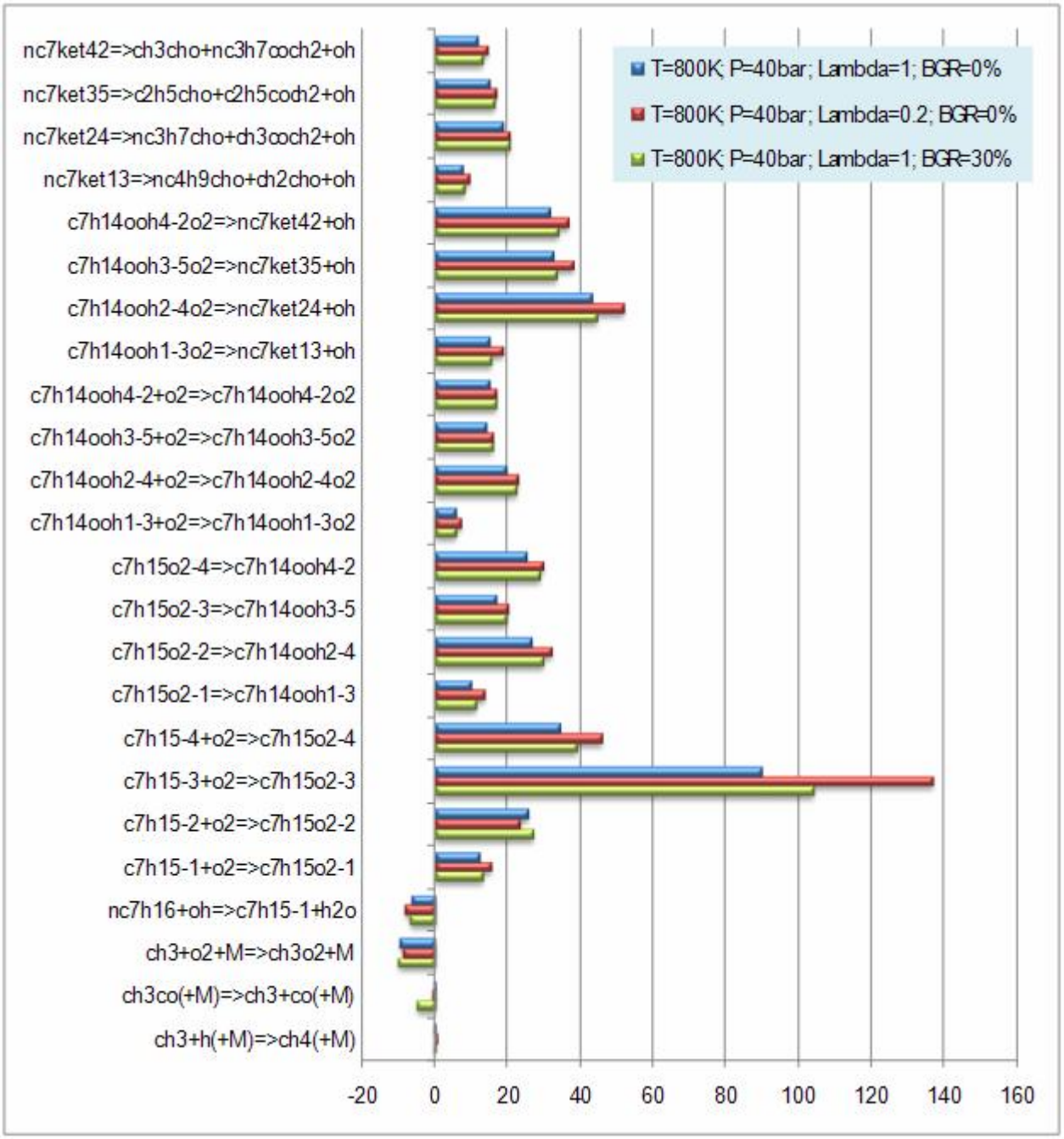

Figure A1. Relative effect of individual reactions on the ignition delay period of n-heptane, %

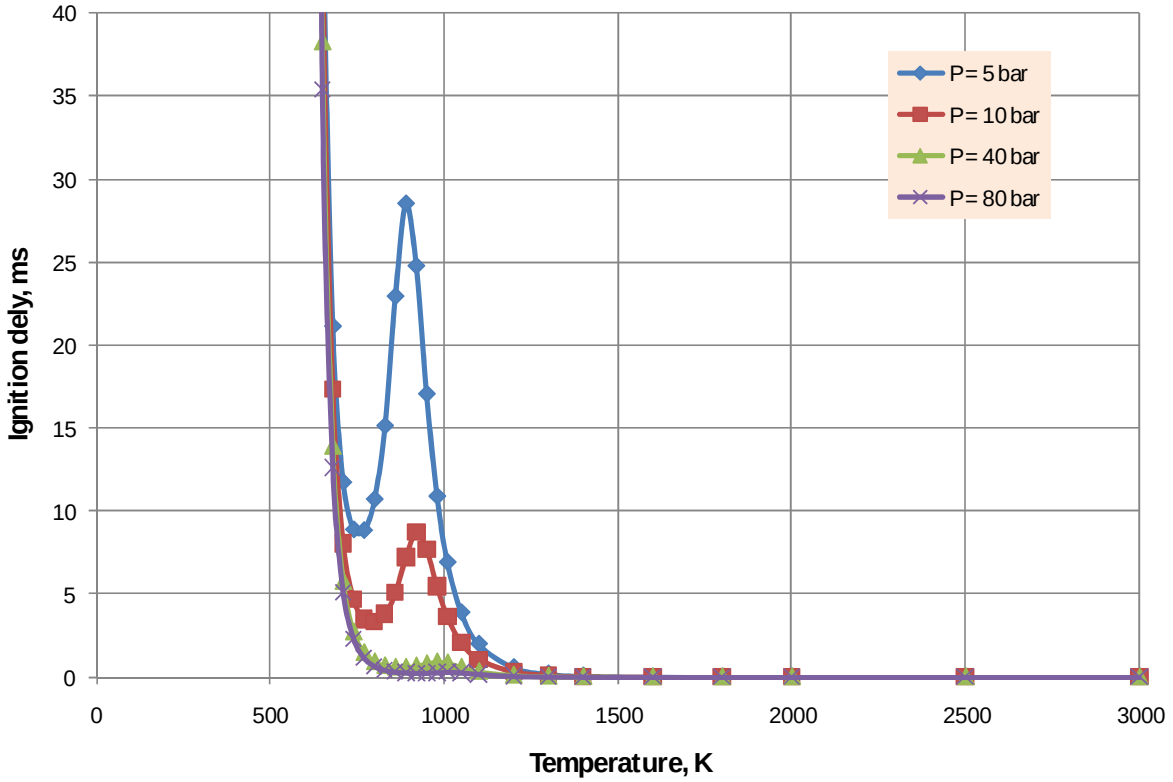

Figure A2. Ignition delay period for n-heptane as a function of the temperature and the pressure at *l* =1 and EGR=0.

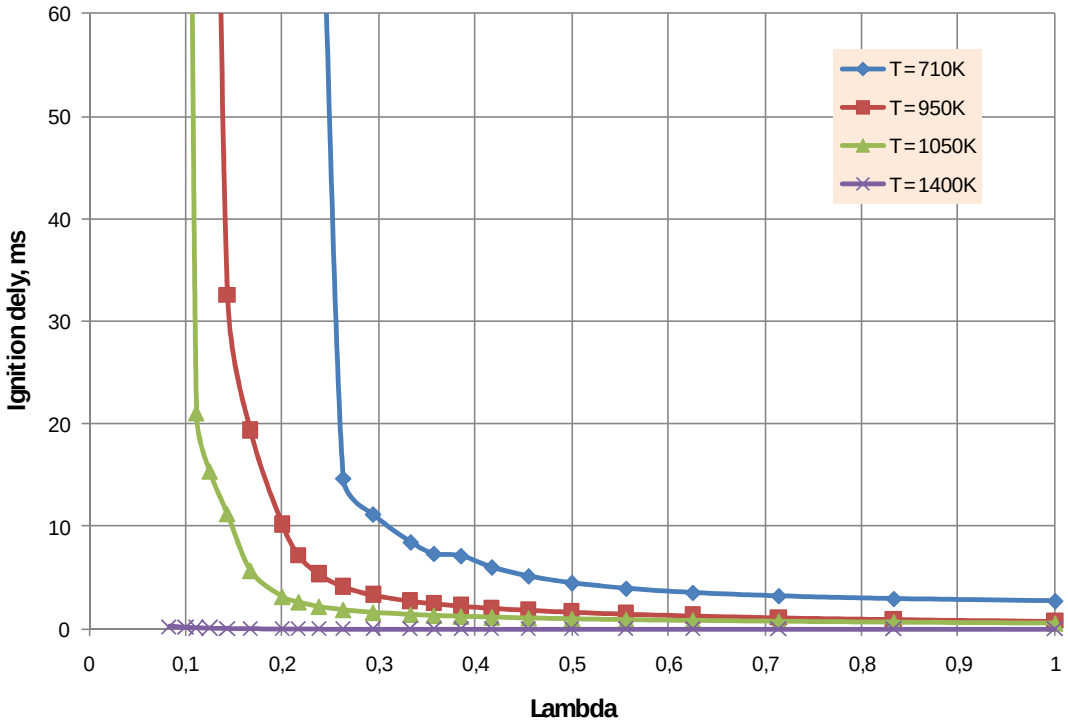

Figure A3. Ignition delay period for n-heptane as a function of the temperature and the composition of the mixture at P=40 bar and EGR=0.

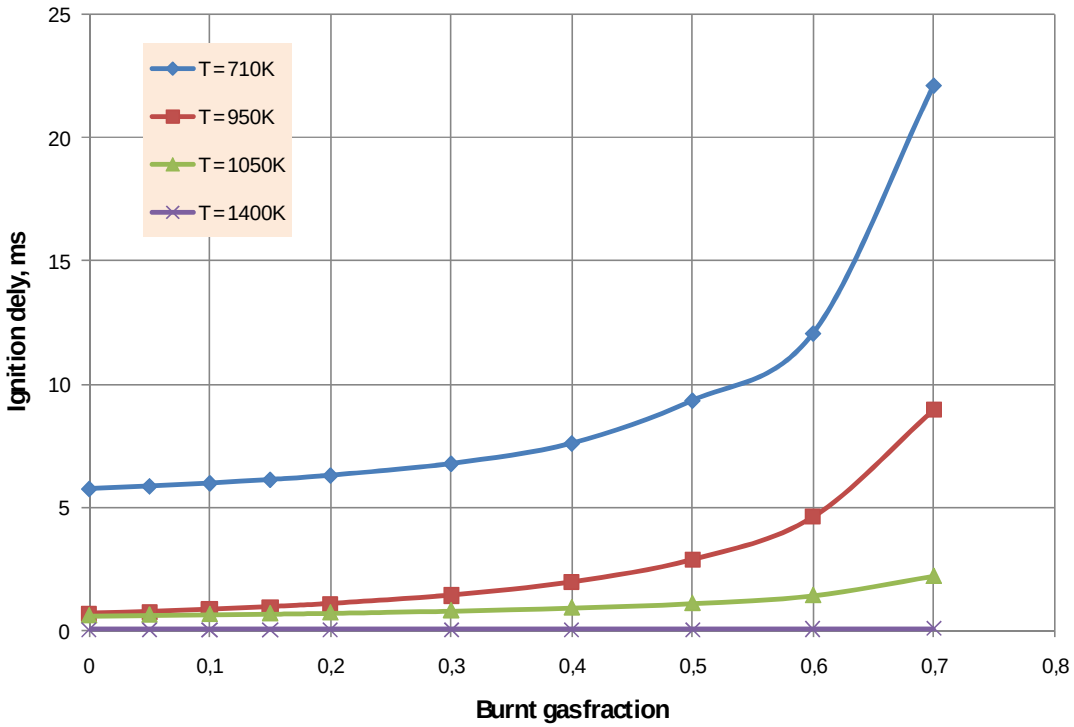

Figure A4. Ignition delay period for n-heptane as a function of the temperature and the fraction of burnt gases in the fresh air-fuel mixture at P=40 and l=1.